Parasitology

cambridge.org/par

Research Article

Cite this article: van der Spuy L, Narciso RB, Hadfield KA, Wepener V, Smit NJ (2025). Exploring South Africa's hidden marine parasite diversity: two new marine *Ergasilus* species (Copepoda: Cyclopoida: Ergasilidae) from the Evileye blaasop, *Amblyrhynchote honckenii* (Bloch). *Parasitology* 1–21. https://doi.org/10.1017/S0031182024001550

Received: 23 August 2024
Revised: 26 October 2024
Accepted: 14 November 2024

Keywords:
28S rDNA; COI mtDNA; Crustacea; marine fish parasite; molecular; phylogenetics; tetraodontid pufferfishes

Corresponding author:
Nico J. Smit;
Email: nico.smit@nwu.ac.za

Exploring South Africa's hidden marine parasite diversity: two new marine *Ergasilus* species (Copepoda: Cyclopoida: Ergasilidae) from the Evileye blaasop, *Amblyrhynchote honckenii* (Bloch)

Linda van der Spuy[1], Rodrigo B. Narciso[1,2], Kerry A. Hadfield[1], Victor Wepener[1] and Nico J. Smit[1]

[1]Water Research Group, Unit for Environmental Sciences and Management, North-West University, Potchefstroom, South Africa and [2]Section of Parasitology, Institute of Biosciences, São Paulo State University (UNESP), Botucatu, São Paulo, Brazil

Abstract

Marine parasites remain understudied in South Africa with little information available on their diversity and the effects these parasites may have on their hosts. This is especially true for parasitic copepods within the family Ergasilidae. Among the 4 genera known in Africa, *Ergasilus* Nordmann, 1832 is the most speciose with 19 reported species. However, this represents only 12% (19/163) of the global diversity. Furthermore, only 5 known African species are reported from marine environments, and only 1 is reported from the South African coastline. Given the rich biodiversity along this coastline, a high marine parasite diversity could be expected from these shores. As a case study, the Evileye blaasop, *Amblyrhynchote honckenii* (Bloch), a marine and brackish fish species, was screened for parasites along the South African coastline. This resulted in the discovery of 2 species of *Ergasilus* new to science (*Ergasilus arenalbus* n. sp. and *Ergasilus chintensis* n. sp.), which makes them the second and third ergasilid species reported for tetraodontid pufferfishes worldwide. Although genetically distinct, the 2 newly described species clustered in the same subclade within the Ergasilidae based on 18S rDNA, 28S rDNA and COI mtDNA phylogenies. The newly described species differ morphologically from each other, and their respective congeners based on the size and armature of the antenna; body segmentation; and general ornamentation throughout the entire body. The addition of these 2 new species from a single host species indicates that South Africa's marine fishes contain most probably a hidden parasitic copepod diversity that is worth exploring.

Introduction

Exploring diversity within marine ecosystems has become increasingly important in recent years, revealing a previously unnoticed level of species richness and genetic variation. This is particularly true for parasitic copepods within the family Ergasilidae Burmeister, 1835 (Boxshall and Defaye, 2008). Among the various genera in this family, *Ergasilus* Nordmann, 1832, stands out as one of the most speciose and widely distributed (Oldewage and van As, 1988; Oldewage and Avenant-Oldewage, 1993; Fikiye *et al.*, 2023; Míč *et al.*, 2023). However, the extent of this diversity remains largely unexplored in Africa (Killian and Avenant-Oldewage, 2013; Fikiye *et al.*, 2023; Míč *et al.*, 2023), with merely 19 reported species, 12% (19/163), of the global diversity (Fikiye *et al.*, 2023; WoRMS, 2024).

The lack of comprehensive studies in Africa limits our understanding of *Ergasilus* diversity, where unique environmental conditions and host communities may foster an even higher diversity of distinct *Ergasilus* species. While some investigations have provided insights into *Ergasilus* species in African freshwater systems (Oldewage and van As, 1988; Fikiye *et al.*, 2023), marine or brackish environments in this region remain largely unexplored, hosting only 5 known species and a single species from the South African coastline (Fikiye *et al.*, 2023; WoRMS, 2024). Additionally, the limited knowledge regarding their diversity and the lack of genetic data, compared to those of other well-studied organisms, hinder comprehensive genomic analyses, creating further challenges in gaining deeper insights into their phylogeny and biology (Fikiye *et al.*, 2023; Míč *et al.*, 2023).

The discovery of new *Ergasilus* species, especially in unexplored regions would aid in filling these crucial gaps and understanding these parasites' biogeography and evolution (Boxshall and Halsey, 2004; Song *et al.*, 2008; Míč *et al.*, 2023). Furthermore, marine regions across the Atlantic and Indian oceans represent hotspots for parasitic diversity due to their wide range of marine habitats (Everett *et al.*, 2015; Miller *et al.*, 2018). Hence, given the rich diversity of *Ergasilus* species described from the southern Atlantic and Indian Ocean regions (see Table 1), South Africa could provide an ideal setting to study marine *Ergasilus* species and

Table 1. Updated information for all marine species of *Ergasilus* Nordmann, 1832 described within the South Atlantic and Indian oceans, with information on host species, host families, distribution and available GenBank data

Species	Host family	Host species	Distribution	Ocean	18S	28S	COI	References
***E. arenalbus* n. sp. present study**	**Tetraodontidae**	**TH: *Amblyrhynchote honckenii* (Bloch)**	**TLOC: Witsand, Breede River Estuary, South Africa**	**South Atlantic**	✓	✓	✓	**Present study**
E. atafonensis Amado and Rocha, 1996	Mugilidae	**TH:** *Mugil curema* Valenciennes, 1836 *M. liza* Valenciennes, 1836; *M. rubrioculus* Harrison *et al.*, 2007; *M. trichodon* Poey, 1875	**TLOC:** Rio de Janeiro, Brazil Sergipe, Brazil; Rio Grande do Sul, Brazil; São Paulo, Brazil; Santos, Brazil; Maranhão, Brazil; Bahia, Brazil	South Atlantic	–	–	–	(Amado and Rocha, 1996)
E. bahiensis Amado and Rocha, 1996	Mugilidae Ariidae	**TH:** *Mugil curema* Valenciennes, 1836 *Sciades herzbergii* (Bloch, 1794)	**TLOC:** Bahia, Brazil Caeté estuary, Brazil; Ajuruteua beach, Brazil	South Atlantic	–	–	–	(Amado and Rocha, 1996; Dos Santos *et al.*, 2021)
E. caraguatatubensis Amado and Rocha, 1996	Mugilidae	**TH:** *Mugil curema* Valenciennes, 1836 *M. liza* Valenciennes, 1836; *M. rubrioculus* Harrison *et al.*, 2007	**TLOC:** Caraguatatuba, Brazil São Paulo, Brazil; Cananeia, Brazil; Rio de Janeiro, Brazil; Maranhão, Brazil	South Atlantic	–	–	–	(Amado and Rocha, 1996)
***E. chintensis* n. sp. present study**	**Tetraodontidae**	**TH: *Amblyrhynchote honckenii* (Bloch)**	**TLOC: Chintsa East, South Africa**	**Indian**	✓	✓	✓	**Present study**
E. cyanopictus Carvalho, 1962	Mugilidae	**TH:** *Mugil cephalus* Linnaeus, 1758	**TLOC:** Rio Nóbrega, Brazil	South Atlantic	–	–	–	(Carvalho, 1962)
E. felichthys (Pearse, 1947) **Syn:** *E. elongatus* Thomsen, 1949	Polyodontidae Ariidae	**TH:** *Bagre marinus* (Mitchill, 1815) *Ariopsis felis* (Linnaeus, 1766); *Genidens barbus* (Lacepède, 1803); *Polyodon spathula* (Walbaum, 1792)	**TLOC**: Beaufort, USA Uruguay; Mobile Bay, USA; St. Louis Bay, USA; Tallapoosa River, USA; Colyell Bay, USA	North Atlantic South Atlantic Gulf of Mexico	–	–	–	(Pearse, 1947; Thomsen, 1949; Johnson and Rogers, 1972)
E. foresti Boxshall *et al.*, 2002	-	Free-living (Plankton nets)	**TLOC:** Piau River estuary, Brazil; Grande do Sul, Brazil	South Atlantic	–	–	–	Boxshall *et al.* (2002)
E. ilani Oldewage and van As, 1988	Mugilidae	**TH:** *Mugil cephalus* Linnaeus, 1758	**TLOC:** Sodwana estuary, Sodwana Bay, KZN, SA	Indian	–	–	–	(Oldewage and van As, 1988)
E. lizae Krøyer, 1863 **Syn:** *E. nanus* Beneden, 1870	Mugilidae Anguillidae Bagridae Cochleae Cyprinodontidae Fundulidae Oxudercidae Sparidae	**TH:** *Mugil liza* Valenciennes, 1836 *Anguilla anguilla* (Linnaeus, 1758); *Acanthopagrus butcheri* (Munro, 1949); *A. australis* (Günther, 1859); *A. berda* (Fabricius, 1775); *Chelon auratus* (Risso, 1810); *C. ramada* (Risso, 1827); *C. saliens* (Risso, 1810); *Coptodon zillii* (Gervais, 1848); *Fundulus similis* (Baird and Girard, 1853); *F. heteroclitus* (Linnaeus, 1766); *Floridichthys carpio* (Günther, 1866); *M. cephalus* Linnaeus, 1758; *M. trichodon*, Poey, 1875; *Mystus gulio* (Hamilton, 1822); *Pseudapocryptes elongatus* (Cuvier, 1816); *Sarotherodon galilaeus* (Linnaeus, 1758); *Trachystoma petardi* (Castelnau, 1875);	**TLOC:** New Orleans, USA Louisiana, USA; Brisbane River, Australia; Texas coast, USA; Georgia coast, USA; Israel; Rio Aconcagua, Chile; La Parguera, Puerto Rico; Melbourne, Australia; Lakes Entrance, Australia; Port Lincoln, Australia; Coffs Harbour, Australia; Gladstone, Australia; Port Canning, India	North Atlantic Pacific Caribbean Mediterranean Gulf of Mexico Indian	–	–	✓	(Beneden, 1870; Byrnes, 1986; Kabata, 1992)
E. myctarothes Wilson, 1913	Sphyrnidae	**TH:** *Sphyrna zygaena* (Linnaeus, 1758)	**TLOC:** Indian Ocean islands	Indian	–	–	–	(Wilson, 1913)
E. pakistanicus Jafri, 1995	Mastacembelidae	**TH:** *Mastacembelus armatus* (Lacepède, 1800)	**TLOC:** Sindh, Pakistan	Indian	–	–	–	(Jafri, 1995)
			TLOC: Veli Lake, India	Indian	–	–	–	Ho *et al.* (1992)

E. parvitergum Ho *et al*., 1992	Cichlidae Carangidae	**TH:** *Etroplus suratensis* (Bloch, 1790); *Carangoides malabaricus* (Bloch and Schneider, 1801)						
E. polynemi Redkar *et al*., 1952	Polynemidae	**TH:** *Eleutheronema tetradactylum* (Shaw, 1804)	**TLOC:** Maharashtra, Mumbai, India	Indian	–	–	–	Redkar *et al*. (1952)
E. rostralis Ho *et al*., 1992	Mugilidae	**TH:** *Planiliza parsia* (Hamilton, 1822) *Osteomugil cunnesius* (Valenciennes, 1836); *P. tade* (Fabricius, 1775); *P. abu* (Heckel, 1843); *P. macrolepis* (Smith, 1846);	**TLOC:** Madras, India Mangalore, Pakistan; Veli Lake, India; Neendakara, India; Shatt Al-Arab River, India	Indian	–	–	–	Ho *et al*. (1992); El-Rashidy and Boxshall (2002)
E. uniseriatus Ho *et al*., 1992	Gobiidae Belonidae	**TH:** *Glossogobius giuris* (Hamilton, 1822) *Xenentodon cancila* (Hamilton, 1822)	**TLOC:** Veli Lake, India Karuvanoor River, India	Indian	–	–	–	Ho *et al*. (1992)
E. vembanadensis Thomas, 1993	Siluridae	**TH:** *Wallago attu* (Bloch and Schneider, 1801)	**TLOC:** Vembanad Lake, India	Indian	–	–	–	(Thomas, 1993)
E. xenomelanirisi Carvalho, 1955	Atherinopsidae	**TH:** *Atherinella brasiliensis* (Quoy and Gaimard, 1825)	**TLOC:** Cananéia, Brazil	South Atlantic	–	–	–	(Carvalho, 1955)
E. youngi Tavares and Luque, 2005	Ariidae	**TH:** *Aspistor luniscutis* (Valenciennes, 1840) *Sciades herzbergii* (Bloch, 1794)	**TLOC:** Angra dos Reis, Brazil Caeté estuary, Brazil	South Atlantic	–	–	–	(Tavares and Luque, 2005; Dos Santos *et al*., 2021)

Information from the present study is represented in bold.
Syn, synonym; TH, type host; TLOC, type locality.

their host associations, possibly yielding a hidden marine parasite diversity within these shores. Understanding the distribution and diversity of *Ergasilus* species across South Africa can provide valuable insights into evolutionary patterns, connectivity between populations and the impact of environmental factors on parasite distribution (Boxshall and Halsey, 2004). Additionally, such comparisons can aid in identifying potential host-switching events and the emergence of novel host–parasite associations (Boxshall and Halsey, 2004; Fikiye *et al.*, 2023; Míč *et al.*, 2023).

This study aimed to start filling this gap by investigating the presence, diversity and molecular characteristics of *Ergasilus* copepods associated with the Evileye blaasop, *Amblyrhynchote honckenii* (Bloch), along the South African coastline. Combining morphological examination and molecular analyses based on partial ribosomal RNA (rRNA) gene regions (18S and 28S), and 1 mitochondrial DNA gene region (COI), 2 new marine *Ergasilus* species were found and described. Revealing and documenting these new species enhances our understanding of the marine parasite diversity within this region, revealing new host–parasite interactions and evolutionary links.

Materials and methods

Sampling

As part of a larger study on the biodiversity of marine fish parasites in southern Africa, 25 *A. honckenii* specimens were collected from 2 coastal localities. Using rod and reel, 15 specimens of *A. honckenii* (13 males and 2 females) were collected from the Breede River Estuary, Witsand (−34.397323; 20.837474) in November 2021 and 10 specimens (1 male, 8 females and 1 juvenile) from the intertidal rocky shore at Chintsa East (−32.836538; 28.116997) in July 2022 (Fig. 1). Following capture, the fish were transported in aerated water containers to a nearby field station for dissection. The specimens were then identified, photographed, weighed, measured and humanely killed using percussive stunning followed by pithing (ethics committee approved standard operation procedure NWU-00267-17-A5). Ethical approval for this project was received from the AnimCare Ethics Committee of the North-West University with ethics number NWU-00565-19-A5. Permits for collecting *A. honckenii* were issued by Cape Nature, Western Cape Province and the South African Department of Agriculture, Forestry and Fisheries (permit no. CN44-87-18289 and RES2022-44, respectively).

Fish were identified using Smith Sea Fishes (Smith and Heemstra, 2012), with fish nomenclature following FishBase (Froese and Pauly, 2024) and Eschmeyer's Catalog of Fishes (Fricke *et al.*, 2024). Host authorities are not included in the text or references.

Morphological analyses

Fish gills were removed and screened for parasites using a Zeiss Stemi 305 compact stereomicroscope (Zeiss, Oberkochen, Germany). Copepod specimens were removed from the gills and preserved in 80% ethanol for morphology and 96% for molecular analysis. Twelve selected specimens underwent morphological observations after being cleared in lactic acid, dissected and temporarily mounted onto slides with glycerine. Photomicrographs of various body structures were captured using a Nikon Y-TV55 video camera mounted on a Nikon ECLIPSE Ni microscope (Nikon, Tokyo, Japan). Image analysis

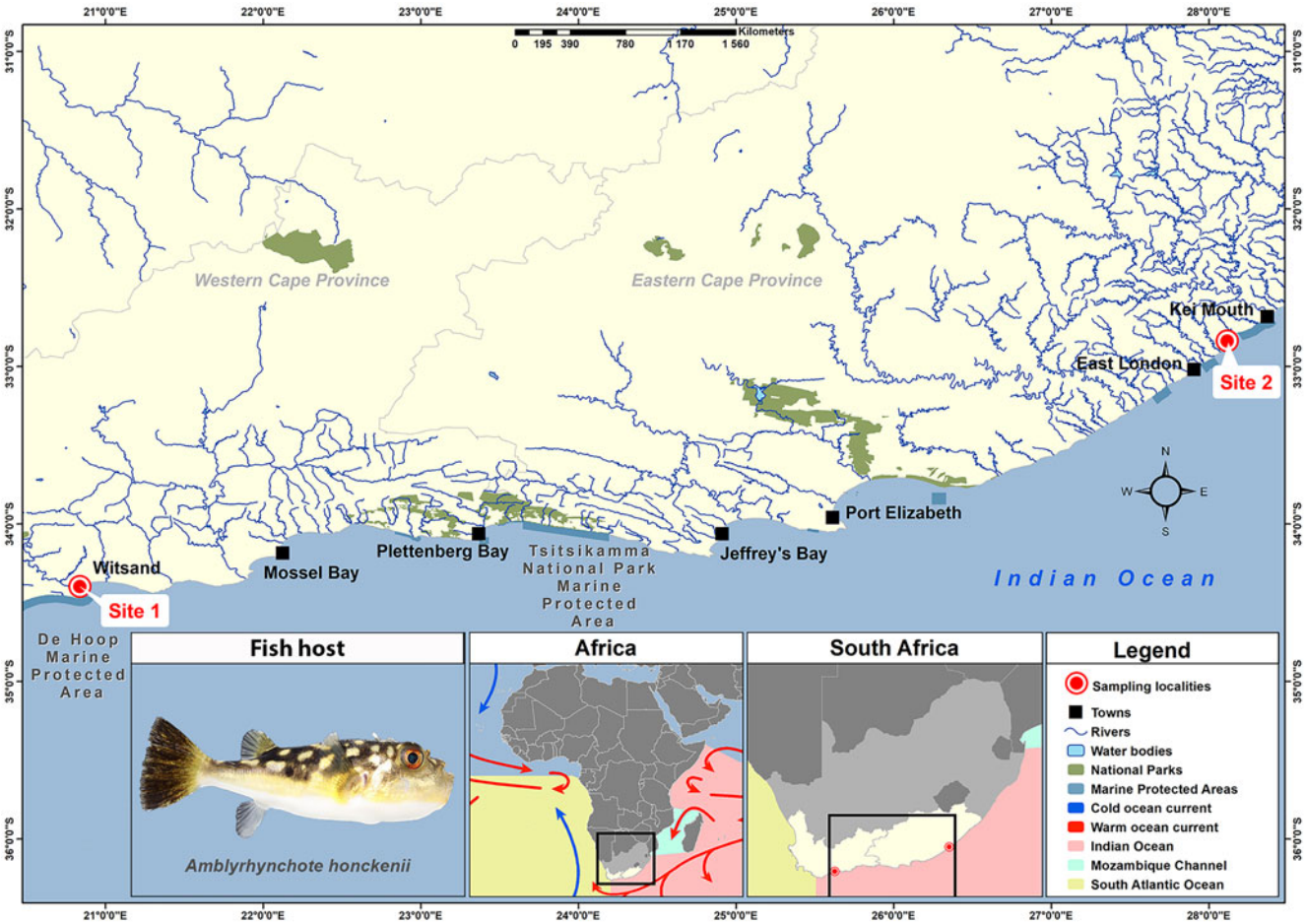

Figure 1. Map indicating the sampling localities of specimens of *Amblyrhynchote honckenii* (Bloch).

https://doi.org/10.1017/S0031182024001550 Published online by Cambridge University Press

software, Image-Pro Express (Nikon), facilitated obtaining all necessary measurements for descriptive analyses. All measurements and terminology for describing body somites and cephalic appendages follow Boxshall and Montú's (1997) guidelines. Measurements are provided in text descriptions and tabular form, with text descriptions including average measurements followed by the range and number of specimens in parentheses. Table 2 presents metrical data as the mean, followed by the standard deviation and the number of specimens examined. Measurements are in micrometres unless otherwise specified. Pencil drawings of specimens and dissected appendages were created using a drawing tube attached to a Nikon ECLIPSE Ni microscope (Nikon). Final digital illustrations were made with Adobe Photoshop version 23.0.1 software using a Wacom Intuos Pro tablet (Wacom, Saitama, Japan).

Furthermore, 6 adult specimens collected from the Breede River Estuary, Witsand, were used for scanning electron microscopy (SEM). SEM could not be performed on specimens from Chintsa East due to the limited availability of specimens. Each specimen selected for SEM observation was cleaned by lightly brushing the surface. Cleaned specimens were dehydrated, placed in hexamethyldisilisane (HMDS), mounted onto carbon tape, placed on aluminium stubs and sputter-coated with carbon (Emscope TB500, Quorum Technologies, Puslinch, ON, USA), followed by 20–30 nm gold/palladium (Eiko IB2 ion coater, Eiko, Japan). Specimens were examined with a FEI Nova NanoSEM 450 scanning electron microscope (FEI, Hillsboro, OR, USA). Images were taken of various characteristic body structures to aid in the morphological description and for comparisons among species.

Molecular analyses

Genomic DNA extraction was conducted using egg strings from 2 copepod specimens from the Breede River Estuary, Witsand, and 1 copepod specimen from Chintsa East. Extraction followed the Macherey-Nagel NucleoSpin® Tissue extraction kit protocol (GmbH and Co. KG, Sandton, South Africa), with an adapted 4 h pre-lysis period and adding 50% more buffer BE. Partial gene amplification targeted 3 gene regions: 2 rRNA gene regions (18S and 28S) and 1 mitochondrial DNA gene region (cytochrome c oxidase I or COI), using primers (18SF, 18SR; 28SF, 28SR) prepared by Song *et al.* (2008) for 18S and 28S, and universal mitochondrial primers (LCO1490 and HCO2198) (Folmer *et al.*, 1994) for COI (Table 3). Amplification reactions were conducted in 25 µL volumes, made up of 12.5 µL of DreamTaq PCR Master Mix (Thermo Fischer Scientific, Waltham, MA, USA), 1.25 µL of 10 µM of each primer, 3 µL of DNA product and 7 µL of double distilled water. Thermocycling conditions followed adapted protocols established by Folmer *et al.* (1994) and Song *et al.* (2008). The PCR thermocycling profile followed adapted conditions: 94°C for 5 min, followed by 40 amplification cycles of 95°C for 30 s, 47°C for 30 s and 72°C for 1 min with a final extension at 72°C for 7 min. Positive PCR products were verified *via* 1% agarose gel electrophoresis and then sent for purification and sequencing in both forward and reverse directions to Inqaba Biotechnical Industries (Pty) Ltd. (Pretoria, South Africa).

Sequences were assembled, aligned, edited and trimmed using Geneious Prime version 2023.1.2 (Biomatters, Auckland, New Zealand). Additionally, the nucleotide Basic Local Alignment Search Tool (BLAST) was used to select *Paracyclopina nana* Smirnov, 1935 (Cyclopettidae Martínez Arbizu, 2000), as the outgroup of the study (Table 4). Considering the limited availability of COI sequences, unpublished sequences of *Ergasilus* species, sourced from the Barcode of Life Database (BOLD), were also included in the COI alignment (Table 4). Alignments for the novel sequences were generated and trimmed using default parameters of MAFFT version 7.4.9 (Katoh *et al.*, 2002; Katoh and Standley, 2013). Genetic divergences among aligned specimens were calculated within Geneious Prime version 2023.1.2, presenting percentage similarities and differences in base numbers.

Table 2. Metrical information of the new species of *Ergasilus* Nordmann, 1832

Character	*Ergasilus arenalbus* n. sp.	*Ergasilus chintensis* n. sp.
Body (L)	1182 ± 137; 12	1035 ± 47; 2
Body (W)	408 ± 49; 12	424 ± 17; 2
Cephalothorax (L)	626 ± 93; 12	608 ± 5; 2
Cephalothorax (W)	397 ± 53; 12	417 ± 6; 2
Cephalosome (L)	336 ± 43; 12	Fused
Cephalosome (W)	387 ± 38; 12	Fused
First pedigerous somite (L)	176 ± 27; 12	Fused
First pedigerous somite (W)	358 ± 42; 12	Fused
Second pedigerous somite (L)	107 ± 24; 12	138 ± 6; 2
Second pedigerous somite (W)	274 ± 31; 12	292 ± 7; 2
Third pedigerous somite (L)	105 ± 18; 12	106 ± 10; 2
Third pedigerous somite (W)	212 ± 37; 12	224 ± 10; 2
Fourth pedigerous somite (L)	61 ± 9; 12	40 ± 3; 2
Fourth pedigerous somite (W)	140 ± 11; 12	112 ± 3; 2
Fifth pedigerous somite (L)	31 ± 6; 12	14 ± 6; 2
Fifth pedigerous somite (W)	80 ± 12; 12	83 ± 16; 2
Genital double somite (L)	135 ± 8; 12	113 ± 4; 2
Genital double somite (W)	109 ± 8; 12	88 ± 3; 2
First abdomen (L)	43 ± 6; 12	28 ± 6; 2
First abdomen (W)	73 ± 8; 12	53 ± 3; 2
Second abdomen (L)	31 ± 6; 12	23 ± 4; 2
Second abdomen (W)	63 ± 3; 12	50 ± 1; 2
Third abdomen (L)	28 ± 4; 12	21 ± 6; 2
Third abdomen (W)	63 ± 2; 12	46 ± 1; 2
Caudal rami (L)	30 ± 2; 12	25 ± 2; 2
Caudal rami (W)	24 ± 1; 12	18 ± 1; 2
Seta I (L)	92 ± 5; 12	61 ± 2; 2
Seta II (L)	77 ± 7; 12	55 ± 2; 2
Seta III (L)	28 ± 5; 12	24 ± 4; 2
Seta IV (L)	282 ± 24; 12	183 ± 3; 2
Antennule (L)	121 ± 8; 12	98 ± 1; 2
Coxobasis (L)	174 ± 23; 12	102 ± 3; 2
Coxobasis (W)	95 ± 10; 12	65 ± 4; 2
First endopodal segment (L)	339 ± 25; 12	184 ± 2; 2
Second endopodal segment (L)	196 ± 15; 12	108 ± 3; 2
Third endopodal segment (L)	28 ± 4; 12	13 ± 2; 2
Claw (L)	161 ± 13; 12	86 ± 3; 2
Eggs (L)	1269 ± 257; 12	1101 ± 4; 2
Eggs (W)	256 ± 42; 12	193 ± 3; 2

L, length; W, width.
Information is presented as the mean, followed by the standard deviation and the number of specimens examined.
All measurements are in micrometres.

https://doi.org/10.1017/S0031182024001550 Published online by Cambridge University Press

Table 3. List of primers used for DNA amplification of parasitic copepods with sequences and references, used to amplify partial 18S, 28S and COI genes in this study

Gene regions	Primers	Sequences	Sources
18S	18SF	5′-AAG GTG TGM CCT ATC AAC T-3′	Song *et al.* (2008)
	18SR	5′-TTA CTT CCT CTA AAC GCT C-3′	
28S	28SF	5′-ACA ACT GTG ATG CCC TTA G-3′	Song *et al.* (2008)
	28SR	5′-TGG TCC GTG TTT CAA GAC G-3′	
COI	LCO1490 (F)	5′-GGTCAACAAATCATAAAGATATTGG-3′	Folmer *et al.* (1994)
	HCO2198 (R)	5′-TAAACTTCAGGGTGACCAAAAAATCA-3′	

The optimal nucleotide substitution model for each dataset was estimated using the Akaike Information Criterion (AIC) in jModelTest 2.1.4 (Posada, 2008; Darriba *et al.*, 2012). The general time-reversible model with invariant sites and gamma-distributed rate variation (GTR + I + G) was recommended for all datasets (18S, 28S and COI). Phylogenetic analyses were performed using Maximum Likelihood (ML) and Bayesian Inference (BI) methods with this suggested model. BI analyses were conducted on the CIPRES Science Gateway version 3.3 (Miller *et al.*, 2010) using MrBayes version 3.2.7a (Ronquist *et al.*, 2012), with 2 independent Markov Chain Monte Carlo (MCMC) runs of 4 chains for 10 million generations, sampling every 1000 generations, and a burn-in of the first 25 000 generations. ML analyses were performed using PhyML version 3.0 (Guindon *et al.*, 2010) on the ATGC bioinformatics platform, with model parameters estimated and 1000 bootstrap repetitions for nodal support. The resulting phylogenetic trees from BI and ML analyses were visualized using TreeViewer version 2.2.0 (Bianchini and Sánchez-Baracaldo, 2024).

Results

Two distinct gill-associated parasitic species, morphologically and molecularly differentiated, were obtained from subsets of 10–15 *A. honckenii* specimens, ranging from 95 to 185 mm in length and weighing 30 to 140 g. Both morphotypes were classified as *Ergasilus* (Ergasilidae) based on specific characteristics, such as body typically cyclopiform with clear segmentation, biramous legs IV with 2-segmented exopods and 3-segmented endopods, 6-segmented antennules, antennas featuring a single claw and the absence of maxillipeds in females, following descriptions by Boxshall and Montú (1997) and Boxshall and Halsey (2004). Notably, only 1 morphotype was found and described from each location, highlighting the uniqueness of both morphotypes in their respective collection sites.

Taxonomy

***Ergasilus arenalbus* n. sp.: Figures 2–5**

ZooBank LSID: urn:lsid:zoobank.org:act:4B5580B2-C5BA-4B8E-99C3-14E9BBF32D3D

Type host: *Amblyrhynchote honckenii* (Bloch) (Tetraodontiformes: Tetraodontidae).

Type locality: Breede River Estuary, Witsand (−34.397323; 20.837474), Western Cape Province, South Africa.

Site on host: Gill filaments.

Prevalence of infection: 67% (10 of 15 pufferfish).

Type material: 151 *Ergasilus* specimens (adult females) were collected. Only adult females were examined: 6 were used for SEM; 2 for dissection; 12 for morphology; and 2 egg strings were used for DNA extraction. The hologenophores (NMB P 1044–NMB P 1045), holotype (NMB P 1042) and 11 paratypes (NMB P 1043) were deposited in the parasitological collections of the National Museum, Bloemfontein, South Africa; the remaining specimens are in the possession of the Water Research Group, North-West University, Potchefstroom, South Africa.

Representative DNA sequences: GenBank accession numbers and numbers of bases (bp) are given as follows: 18S: 1333 and 1344 bp long sequences of 2 specimens, accession numbers: PQ451954 and PQ451956; 28S: 668 and 664 bp long sequences of 2 specimens, accession numbers: PQ451957 and PQ451958; and COI: 701 bp long sequence of 1 specimen, accession number: PQ439339.

Etymology: The species name '*arenalbus*' is derived from 'arena albus' meaning white sand (English) or wit sand (Afrikaans) in Latin. This refers to 'Witsand' the name of the type locality of this species.

Description

Adult female description (based on 12 specimens). Body length (measured from the anterior margin of cephalosome to posterior margin of caudal rami) 1182 (959–1370; $n = 12$). Body comprises prosome, urosome and caudal rami. Prosome 5-segmented, composed of cephalosome and 4 free pedigerous somites. Cephalothorax composed of cephalosome and first pedigerous somite; cephalosome separated dorsally from previous somite by flexible cuticle (Figs 2A and 5A). Cephalosome slightly shorter than wide, 336 (272–414; $n = 12$) long by 387 (316–460; $n = 12$) wide, oval to trapezoidal, with antennules and antenna visible in dorsal view. Cephalic ornamentation comprising of anterior circular eyespot and inverted T-shaped mark of thickened chitin situated medially on dorsal side (Fig. 2A and B). Paired sensory pores and papillae observed anterior to eyespot with numerous sensory papillae and pores scattered over dorsal surface of cephalosome. Rostrum well-developed, with truncated posterior margin. All pedigerous somites wider than long and progressively smaller. Paired sensory papillae observed mid-dorsally on segments 2–5. First pedigerous somite 176 (129–218; $n = 12$) long by 358 (297–428; $n = 12$) wide; second pedigerous somite 107 (82–154; $n = 12$) long by 274 (241–334; $n = 12$) wide; third pedigerous somite 105 (78–138; $n = 12$) long by 212 (163–268; $n = 12$) wide; fourth pedigerous somite 61 (44–82; $n = 12$) long by 140 (127–169; $n = 12$) wide.

Urosome comprising reduced fifth pedigerous somite, genital double somite and 3 free abdominal somites (Fig. 3A). Reduced fifth pedigerous somite 31 (20–39; $n = 12$) long by 80 (72–114; $n = 12$) wide. Genital double-somite longer than wide, 135 (120–152; $n = 12$) long by 109 (100–130; $n = 12$) wide (Fig. 3A), bearing a pair of multiseriate egg sacs dorsally (Figs 2A and 4A), measuring 1269 (989–1662; $n = 12$) long by 256 (222–340; $n = 12$) wide (Figs 2A and 4A). Abdomen 3-segmented; first abdominal somite widest, 43 (36–56; $n = 12$) long by 73 (64–92; $n = 12$) wide; second abdominal somite shorter, 31 (23–40; $n =$

https://doi.org/10.1017/S0031182024001550 Published online by Cambridge University Press

Table 4. List of GenBank and Barcode of Life Database (BOLD) Ergasilidae sequences included in the phylogenetic analyses

Taxon	Host	Locality	GenBank accession numbers			References
			18S	28S	COI	
Acusicola margulisae	*Amphilophus citrinellus*; *Parachromis managuensis*; *Oreochromis* sp.; *Poecilia exicana*	Nicaragua	MN852694 MN 852695	MN852849 MN852850	MN854868 MN854869	Santacruz *et al.* (2020)
Dermoergasilus madagascarensis	*Paretroplus*; *polyactis*	Madagascar	PP115568 –	PP115569 –	PP117931 PP117932	Míč *et al.* (2024)
Ergasilus anchoratus	*Pseudobagrus fulvidraco*	China	DQ107564	DQ107528	–	Song *et al.* (2008)
***Ergasilus arenalbus* n. sp.**	***Amblyrhynchote honckenii***	**South Africa**	**PQ451954 PQ451956**	**PQ451957 PQ451958**	**PQ439339** –	**Present study**
**Ergasilus auritus*	*Gasterosteus aculeatus*	Canada	–	–	ECTCR091-14	BOLD
Ergasilus briani	*Misgurnus anguillicaudatus*	China	DQ107572	DQ107532	–	Song *et al.* (2008)
Ergasilus caparti	*Neolamprologus brichardi*	Burundi	OQ407469	OQ407474	–	Míč *et al.* (2023)
***Ergasilus chintensis* n. sp.**	***Amblyrhynchote honckenii***	**South Africa**	**PQ451955**	**PQ451959**	**PQ439340**	**Present study**
Ergasilus hypomesi	*Acanthogobius hasta*	China	DQ107573	DQ107539	–	Song *et al.* (2008)
**Ergasilus lizae*	*Fundulus diaphanus*	Canada	–	–	ECTCR024-14	BOLD
Ergasilus macrodactylus	*Gnathochromis permaxillaris*	Burundi	OQ407465	OQ407470	–	Míč *et al.* (2023)
Ergasilus megacheir	*Simochromis diagramma*	Burundi	OQ407466	OQ407471	–	Míč *et al.* (2023)
Ergasilus mirabilis	*Clarias gariepinus*	South Africa Zambia	OR449753 OR449754	OR449755 OR449756	OR448769 OR448770	Fikiye *et al.* (2023)
Ergasilus parasarsi	*Simochromis diagramma*	Burundi	OQ407467	OQ407473	–	Míč *et al.* (2023)
Ergasilus parvus	*Spathodus erythrodon*	Burundi	OQ407468	OQ407472	–	Míč *et al.* (2023)
Ergasilus parasiluri	*Tachysurus fulvidraco*	China	DQ107567	DQ107536	–	Song *et al.* (2008)
Ergasilus peregrinus	*Siniperca chuatsi*	China	DQ107577	DQ107531	–	Song *et al.* (2008)
Ergasilus scalaris	*Tachysurus dumerili*	China	DQ107565	DQ107538	–	Song *et al.* (2008)
Ergasilus sieboldi	*Perca fluviatilis*; *Sparus aurata*	Czech Republic	MW810238	MW810242	–	Kvach *et al.* (2021)
Ergasilus tumidus	*Acanthorhodeus taenianalis*	China	DQ107569 DQ107570	DQ107533 DQ107534	– –	Song *et al.* (2008)
Ergasilus wilsoni	Free-living	South Korea	KR048765	KR048843	KR049036	Baek *et al.* (2016)
Ergasilus yaluzangbus	*Gymnocypris stewartii*	China	DQ107578	DQ107540	–	Song *et al.* (2008)
Neoergasilus japonicus	*Lepomis gibbosus* *Scardinius erythrophthalmus*	Czech Republic USA	MH167970 MW810236 – –	MH167968 MW810240 – –	– – MZ964935 MZ964938	Ondračková *et al.* (2019), Kvach *et al.* (2021), Vasquez *et al.* (2023)
Paraergasilus brevidigitus	*Cyprinus carpio*	China	DQ107576	DQ107530	–	Song *et al.* (2008)
Paraergasilus longidigitus	*Abramis brama*; *Perca fluviatilis*; *Scardinius erythrophthalmu*	Czech Republic	MW810239	MW810243	–	Kvach *et al.* (2021)
Paraergasilus medius	*Ctenopharyngodon idellus*	China	DQ107574	DQ107529	–	Song *et al.* (2008)
Sinergasilus major	*Ctenopharyngodon Idella* *Silurus glanis*	China Hungary	DQ107558 –	– MZ047815	– –	Song *et al.* (2008) Dos Santos *et al.* (2021)
Sinergasilus polycolpus	*Hypophthalmichthys molitrix*	China	DQ107563	DQ107525	–	Song *et al.* (2008)
Sinergasilus undulatus	*Cyprinus carpio*	China	DQ107561 –	DQ107526 –	– MW080644	Song *et al.* (2008) Hua *et al.* (2021)
**Thersitina gastorostei*	*Gasterosteus aculeatus*	Canada	–	–	ECTCR063-14	BOLD
Paracyclopina nana	Free-living	Korea	– FJ214952	– FJ214952	EU877959 –	Ki *et al.* (2009) Ki *et al.* (2011)

The taxa in bold fonts are sequences generated from the present study. *Paracyclopina nana* (in the grey shade) was used as the outgroup.
**Taxon from the Barcode of Life Database (BOLD).

https://doi.org/10.1017/S0031182024001550 Published online by Cambridge University Press

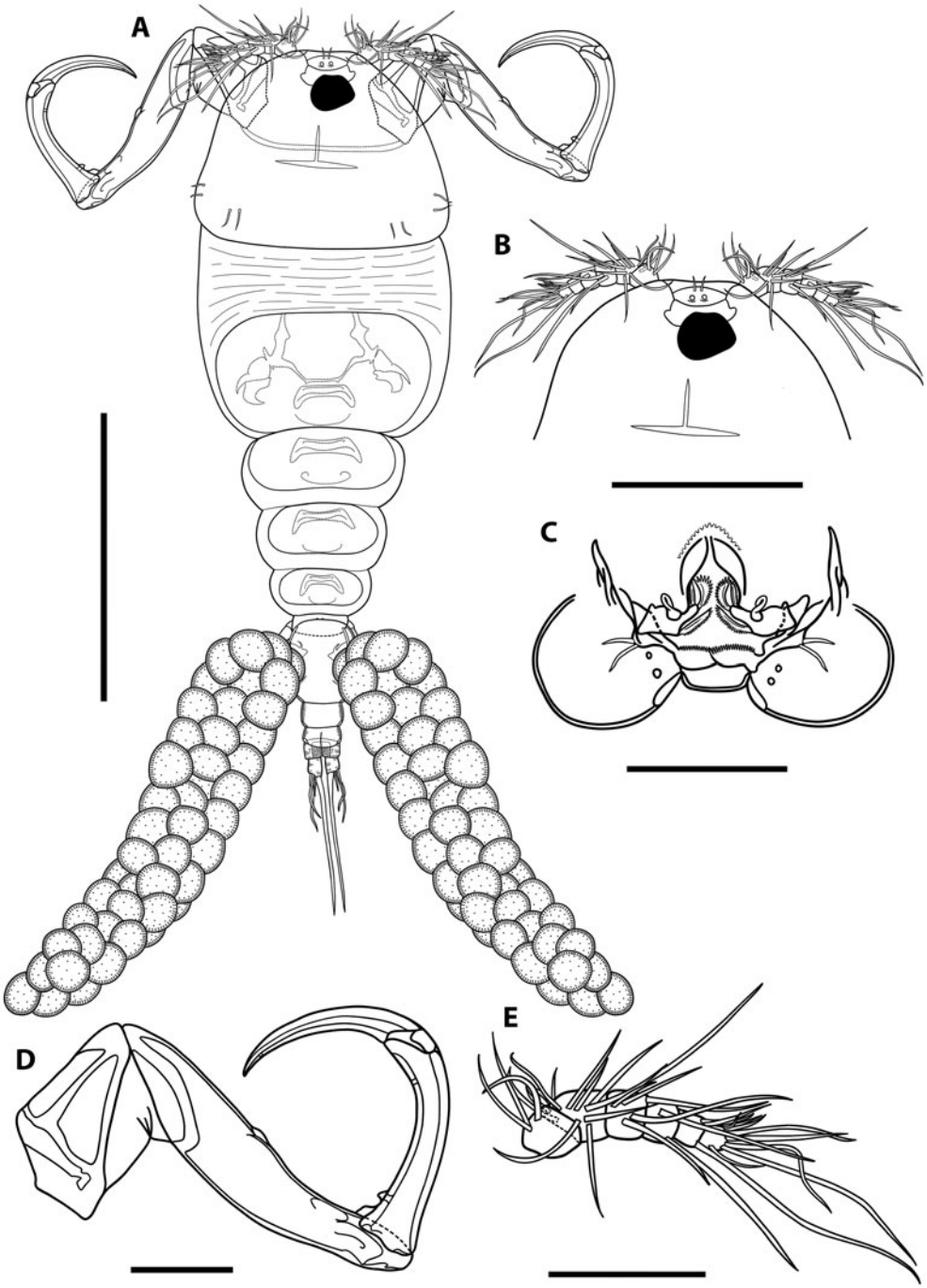

Figure 2. Illustrations of adult female of *Ergasilus arenalbus* n. sp: (A) entire specimen, dorsal view; (B) detail of cephalosome, dorsal view; (C) mouth, mandible, maxillule and maxilla; (D) antenna; (E) antennule. Scale bars: A – 500 μm; B – 250 μm; C–E – 100 μm.

12) long by 63 (55–67; $n = 12$) wide; third somite (= anal somite) incised dorsoventrally (= anal opening or anus) forming attachment for caudal rami, 28 (22–32; $n = 12$) long by 63 (59–68; $n = 12$) wide, ornamented with pair of pores on dorsal side; each pore located laterally to anal opening and carrying bristle (Figs 3A, 4E, 5C). All abdominal somites with posterior row of ventral spinules (Figs 4E and 5C).

Caudal rami slightly elongated, 30 (26–33; $n = 12$) long by 24 (22–28; $n = 12$) wide, with 4 setae (Fig. 3A). Innermost seta (IV) longest 282 (226–308; $n = 12$), followed by shortest seta (III) 28 (20–39; $n = 12$) and 2 longer setae (II and I) 77 (60–87; $n = 12$) and 92 (83–99; $n = 12$), respectively (Fig. 3A).

Antennule 6-segmented, armed with long and short setae (Fig. 2E). Setal formula from proximal to distal segments given as 3–12–6–2–3–8 (total 34). Antenna 4-segmented (Figs 2D and 4B) comprising coxobasis, 174 (110–196; $n = 12$) long by 95 (73–114; $n = 12$) wide; and 3-segmented endopod; armed with curved terminal claw (Figs 2D and 4B). First endopod segment longest 339 (288–366; $n = 12$), followed by second endopod segment 196 (152–215; $n = 12$) and small third endopod segment 28 (24–40; $n = 12$). Prominent spine observed on anterior second endopod segment (Figs 2D, 4B, 5D). Terminal claw pointed and smooth 161 (127–186; $n = 12$), with fossa on concave margin.

Mouth positioned ventrally on cephalosome. Labrum with internal teeth; teeth arranged in an arch. Mandible armed with 3 blades (anterior, medial and posterior blades); anterior blade thinner and shorter than others, ornamented along anterior margin; medial and posterior blades, both with teeth on opposite

https://doi.org/10.1017/S0031182024001550 Published online by Cambridge University Press

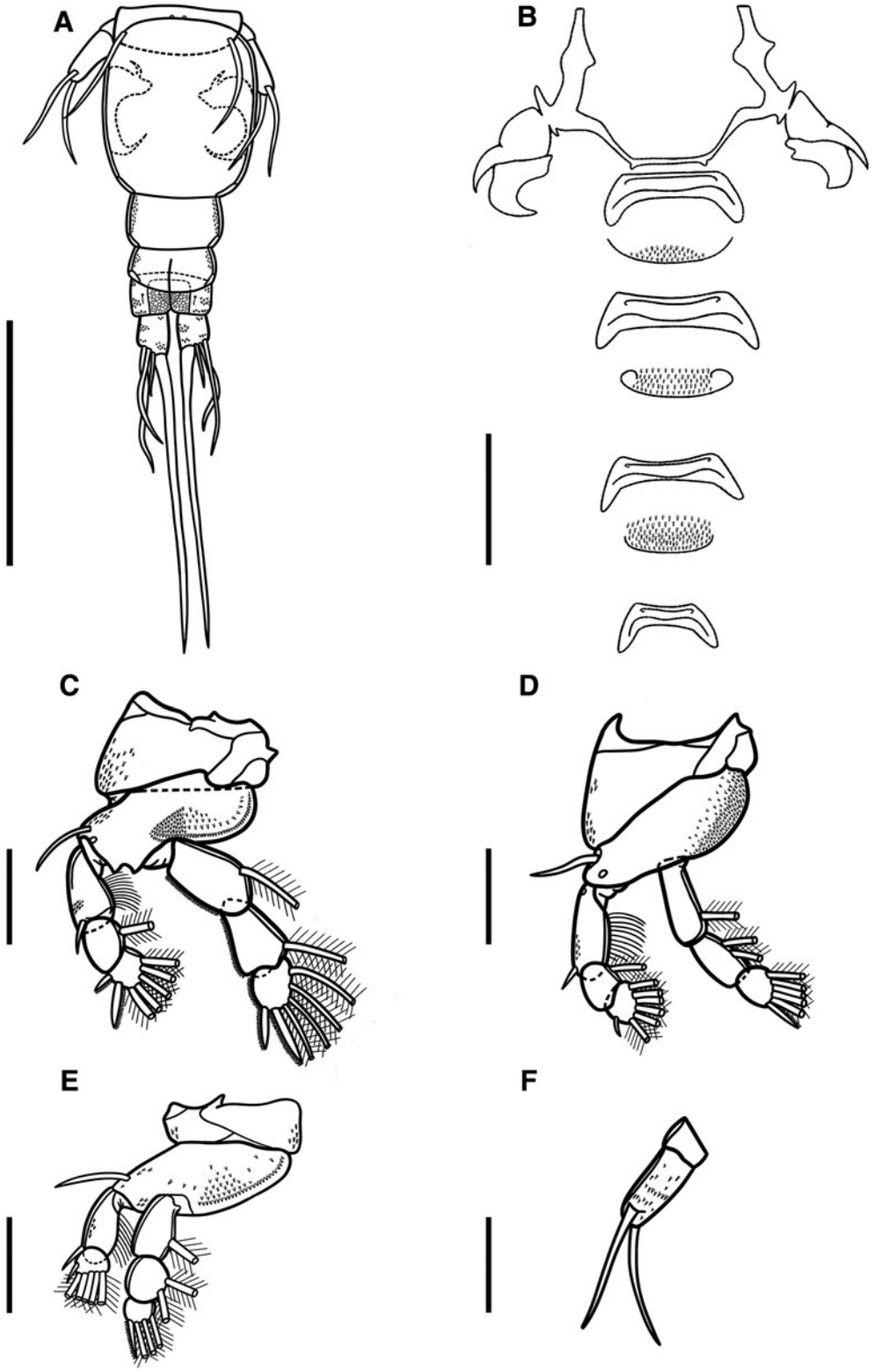

Figure 3. Illustrations of adult female of *Ergasilus arenalbus* n. sp: (A) urosome, dorsal view; (B) intercoxal sclerites and interpodal plates; (C) leg 1; (D) leg 2 and leg 3; (E) leg 4; (F) leg 5. Scale bars: A – 200 μm; B – 100 μm; C–F – 50 μm.

margin. Maxillule armed with 2 unequal setae; innermost seta shortest; ornamented with 1 pore and multiple spinules; pore lacking bristle (Fig. 2C). Maxilla 2-segmented, comprising syncoxa (= first segment) and basis (= second segment); syncoxa broad, with 2 distal pores; basis ornamented with multiple spinules on posterior margin. Labium broad, unornamented; midregion produced posteriorly, with truncated posterior margin.

Swimming legs I to IV; each comprising coxa, basis and 2 segmented rami (i.e. exopod, endopod). Rami of all legs 3-segmented, except 2-segmented exopod of leg IV. Segments distinct, typical with similar basic morphology as in other species of *Ergasilus*. Armature on rami as Roman and Arabic numerals indicating spines and plumose setae, respectively, in Table 5.

Leg I (Fig. 3C). Coxa ornamented with spinules on outer margin. Basis armed with bare outer seta, ornamented with spinules on both sides; posterior margin protrudes posteriorly forming 1 spinous process; spines located between rami (Figs 3C and 4C). Exopod 3-segmented; first endopodal segment with distal spine,

https://doi.org/10.1017/S0031182024001550 Published online by Cambridge University Press

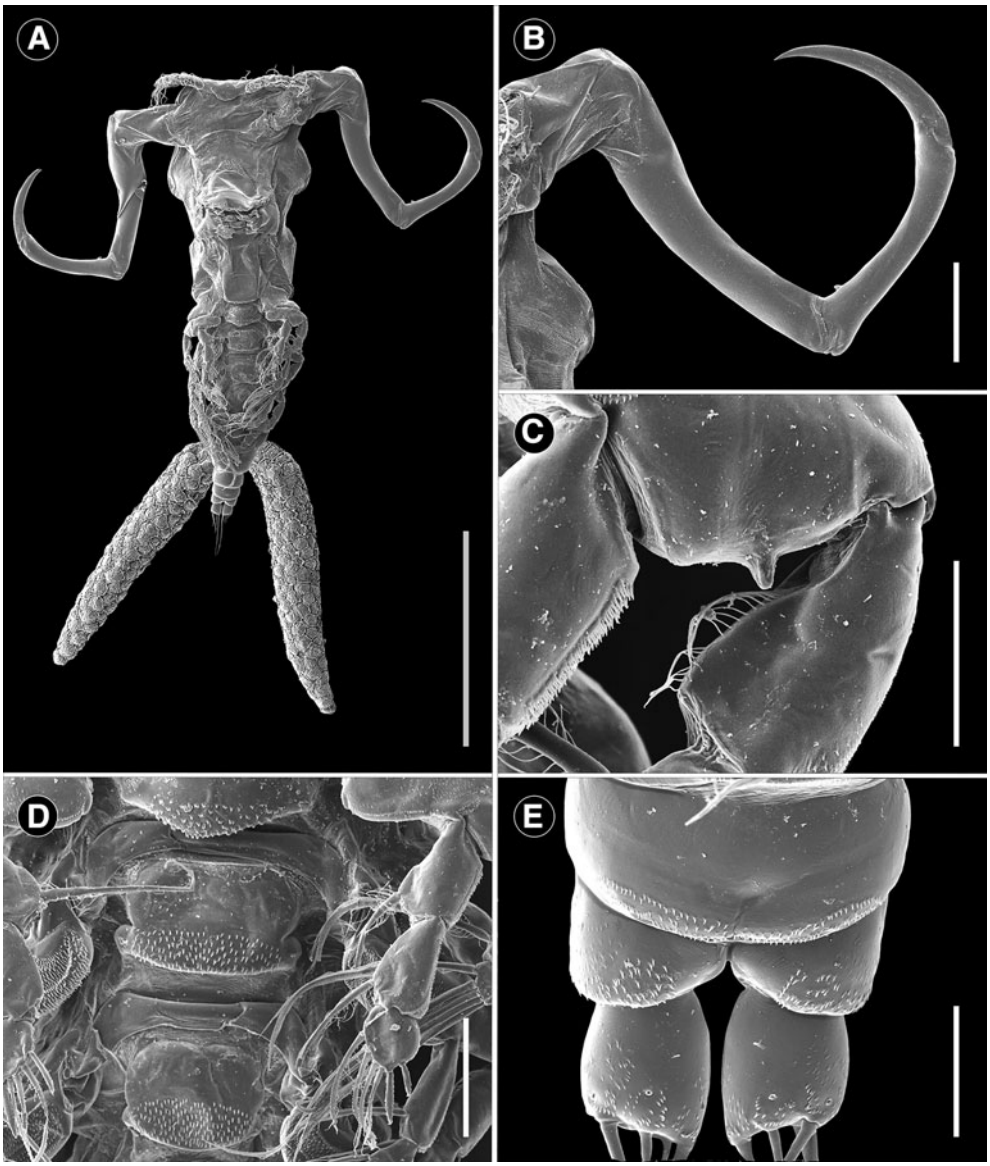

Figure 4. Scanning electron microscope photomicrographs of adult female *Ergasilus arenalbus* n. sp. showing features from the ventral and dorsal view: (A) entire specimen; (B) antenna; (C) base of first leg; (D) ventral view of interpodal plates; (E)– dorsal view of ornamentation on caudal rami. Scale bars: A – 500 μm; B – 100 μm; C–E – 25 μm.

ornamented with patch of spinules on outer margin; spinules located just above distal spine; and bristles along outer margin; second exopodal segment with 1 plumose seta, unornamented; third exopodal segment armed with 2 serrated spines (inner and outer spine); inner spine about 2.0 times longer than outer spine; and 5 plumose setae. Endopod 3-segmented; all segments with spinules along inner margin; first and second endopodal segment, each with 1 plumose seta on inner margin; third endopodal segment armed with 2 serrated spines (inner and outer spine); inner spine about 2.0 times longer than outer spine; and 4 plumose setae.

Leg II (Fig. 3D). Coxa ornamented with spinules on outer margin. Basis armed with bare outer seta, ornamented with spinules on both sides. Exopod 3-segmented; first exopodal segment with distal spine, ornamented with patch of spinules on outer margin; spinules located just above distal spine; and bristles along inner margin; second exopodal segment armed with 1 plumose seta; third exopodal segment with simple spine (or non-serrated) and 6 plumose setae. Endopod 3-segmented; first and second endopodal segments with 1 and 2 plumose setae, respectively; third endopodal segment with serrated spine and 4 plumose setae. Leg III with the same armament and ornamentation described for leg II.

Leg IV (Fig. 3E). Coxa ornamented with spinules on both sides. Basis armed with bare outer seta, with spinules scattered across surface. Exopod 2-segmented; first exopodal segment armed with distal spine, ornamented with spinules and bristles on outer and inner margin, respectively; second exopodal segment with 1 spine and 5 plumose setae. Endopod 3-segmented, all segments lacking ornaments on both margins; first and second endopodal segment with 1 and 2 plumose setae, respectively; third endopodal segment with 1 serrated spine and 3 plumose setae.

Leg V (Fig. 3F) with single ramus. Ramus 2-segmented; proximal segment rectangular, without any armaments or ornaments; distal segment about 3.0 times longer than previous segment, with spinules scattered across surface, armed with 2 bare setae.

Intercoxal sclerites and interpodal plates of all legs, present (Figs 2A, 3B, 4D). Intercoxal sclerites unornamented, with both ends directed posteriorly. Interpodal plates present; first to third plate with spinules; fourth plate absent (Figs 2A and 3B).

https://doi.org/10.1017/S0031182024001550 Published online by Cambridge University Press

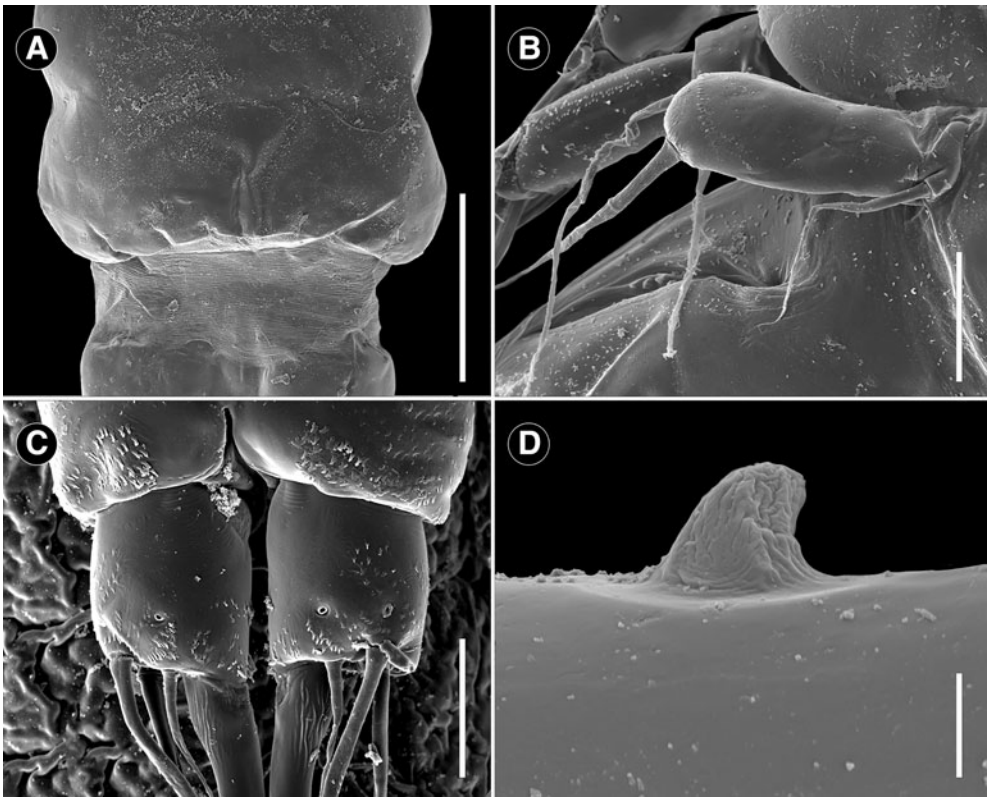

Figure 5. Scanning electron microscope photomicrographs of adult female *Ergasilus arenalbus* n. sp showing features from the ventral and dorsal view: (A) detail of the cuticular membrane of cephalothorax; (B) leg 5; (C) ventral view of detail of the caudal rami; (D) detail of the spine of the third antennal segment. Scale bars: A – 150 µm; B – 25 µm; C – 20 µm; D – 5 µm.

Table 5. Spine–setae formula on swimming legs of *Ergasilus arenalbus* n. sp.

	Coxa	Basis	Exopod	Endopod
Leg I	0-0	0-1	I-0; 0-1; II-5	0-1; 0-1; II-4
Leg II	0-0	0-1	I-0; 0-1; I-6	0-1; 0-2; I-4
Leg III	0-0	0-1	I-0; 0-1; I-6	0-1; 0-2; I-4
Leg IV	0-0	0-1	I-0; I-5	0-1; 0-2; I-3

Number of spines in Roman numerals, number of setae in Arabic numerals.

Remarks

The detailed morphological description of *E. arenalbus* n. sp. sheds light on its distinctiveness among the recognized species of *Ergasilus* worldwide. With 163 valid species known, comparisons were only made with other marine *Ergasilus* species from the southern Atlantic and Indian Ocean regions. Among the 17 marine species from these regions (Table 1), *E. arenalbus* n. sp. stands out in several key morphological aspects, notably in size; armature of the antenna; the segmentation in the body (free *vs* fused prosome somites); and general ornamentation throughout the entire body. Firstly, its larger body size, with a length averaging 1182 µm, sets it apart from species such as *E. atafonensis* Amado and Rocha, 1996, *E. bahiensis* Amado and Rocha, 1996, *E. caraguatatubensis* Amado and Rocha, 1996, *E. ilani* Oldewage and van As, 1988, *E. myctarothes* Wilson, 1913, *E. parvitergum* Ho *et al.*, 1992, *E. rostralis* Ho *et al.*, 1992 and *E. uniseriatus* Ho *et al.*, 1992 which typically have a smaller total length, below 1054 µm. Conversely, *E. felichthys* (Pearse, 1947) and *E. youngi* Tavares and Luque, 2005 present larger body sizes, approximately 1400 µm, emphasizing the distinctive size range of the newly described species. The segmentation of the body, particularly the free *vs* fused prosome somites, is another distinguishing factor. For instance, *E. arenalbus* n. sp. shows variations in abdominal somite dimensions, contrasting with the more uniform structures seen in species like *E. atafonensis*. This variability extends to cephalosome characteristics, with *E. caraguatatubensis* exhibiting an inflated shape absent in *E. arenalbus* n. sp. The spine-setae formulae on the swimming legs of *E. arenalbus* n. sp. further differentiate it, particularly when compared to all other marine congeners, except for *E. lizae* Krøyer, 1863. *Ergasilus atafonensis*, *E. bahiensis*, *E. myctarothes*, *E. parvitergum* and *E. xenomelanirisi* Carvalho, 1955, have a spine on the outer margin of the second exopodite of leg I, which is absent in the new species. In addition, *E. ilani* lacks a certain number of armaments that are common on the legs of the species in the group, for example, spines and setae on the first segments of the exopod and endopod, respectively. In *E. caraguatatubensis*, *E. felichthys*, *E. foresti* Boxshall *et al.*, 2002, *E. ilani*, *E. parvitergum* and *E. youngi*, leg V is extremely reduced and is represented by 1 or 2 setae. While the setae formula of the antennule is also a clear distinguishing factor, species like *E. ilani*, *E. rostralis* and *E. uniseriatus* were further excluded due to their antennules being described as only 5-segmented, unlike the 6-segmented antennules observed in the other *Ergasilus* species. Although *E. arenalbus* n. sp. morphologically resembles *E. lizae* in many aspects, it differs notably in the armature of the antenna, with *E. arenalbus* n. sp. exhibiting a single spine on the anterior second endopod segment, unlike *E. lizae*. Additionally, a distinctive feature of the new species is the spine projections on the posterior margin of the basis of the first leg, a characteristic absent in all other species examined. This comprehensive morphological analysis of *E. arenalbus* n. sp. provides a clear understanding of its unique features within the *Ergasilus* genus, emphasizing size, body segmentation, appendage armature and ornamentation as crucial factors in species differentiation.

https://doi.org/10.1017/S0031182024001550 Published online by Cambridge University Press

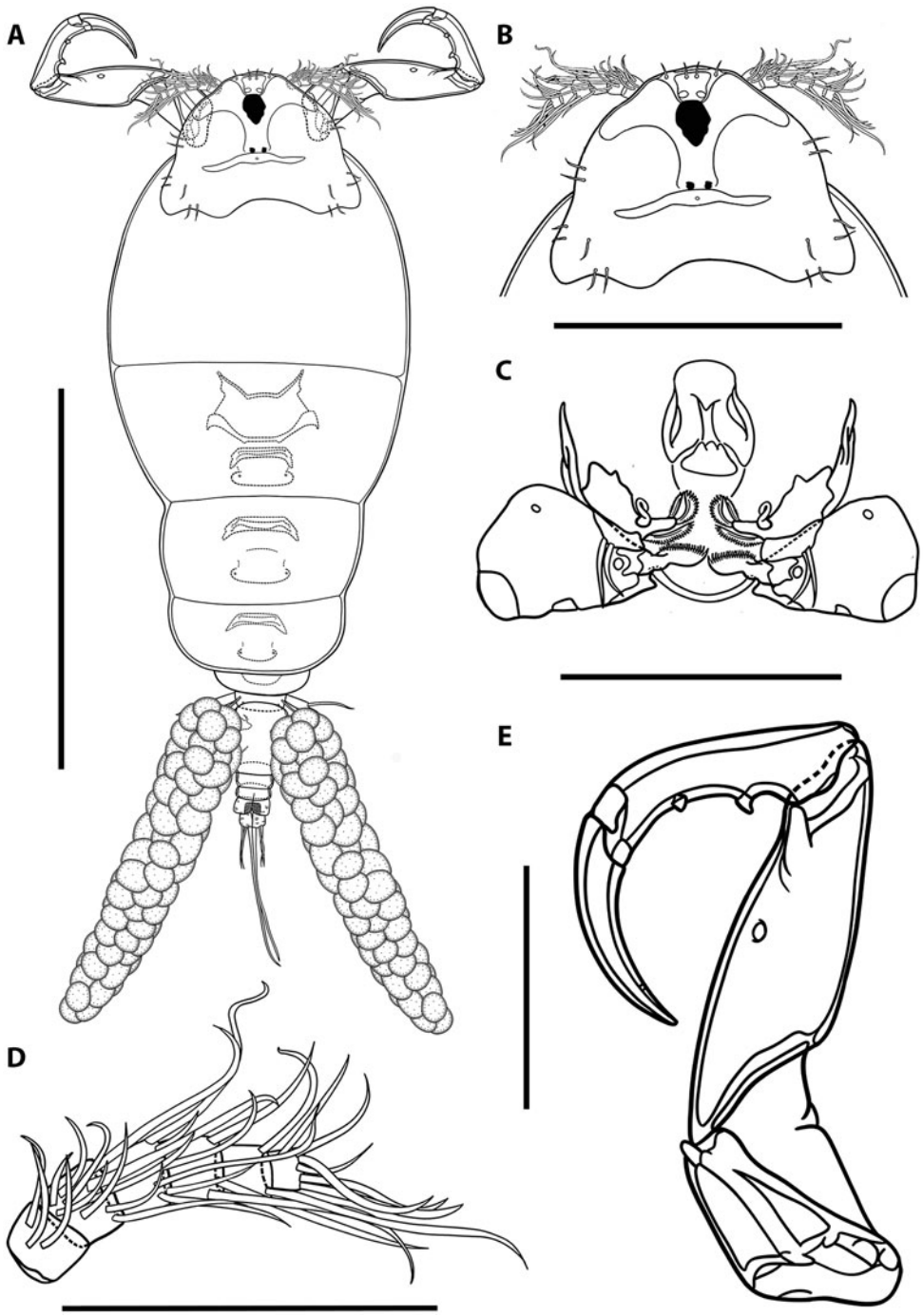

Figure 6. Illustrations of adult female of *Ergasilus chintensis* n. sp: (A) entire specimen, dorsal view; (B) detail of the cephalosome, dorsal view; (C) mouth, mandible, maxillule and maxilla; (D) antennule; (E) antenna. Scale bars: A – 500 μm; B – 250 μm; C–E – 100 μm.

Ergasilus chintensis n. sp.: Figures 6–7

ZooBank LSID: urn:lsid:zoobank.org:act:E51F54EC-9CF7-47DA-B4B7-61DEC73B430F.

Type host: *Amblyrhynchote honckenii* (Bloch) (Tetraodontiformes: Tetraodontidae).

Type locality: Chintsa East (−32.836538; 28.116997), Eastern Cape Province, South Africa.

Site on host: Gill filaments.

Prevalence of infection: 20% (2 of 10 pufferfish observed).

Type material: 2 ergasilids (adult females) were collected. Only adult females were examined: 2 were used for morphology, and 1 egg string was used for DNA extraction. The hologenophore (NMB P 1047) and holotype (NMB P 1046) were deposited in the parasitological collections of the National Museum, Bloemfontein, South Africa.

Representative DNA sequences: GenBank accession numbers and numbers of bases (bp) are given as follows: 18S: 1353 bp long sequence of 1 specimen, accession number: PQ451955; 28S: 668 bp long sequence of 1 specimen, accession number: PQ451959; and COI: 692 bp long sequence of 1 specimen, accession number: PQ439340.

Etymology: The species name '*chintensis*' is derived from Chintsa, representing the type locality of the species.

Description

Adult female description (based on 2 specimens). Body length (measured from the anterior margin of cephalosome to the posterior margin of caudal rami) 1035 (1002–1068; $n = 2$). Body

https://doi.org/10.1017/S0031182024001550 Published online by Cambridge University Press

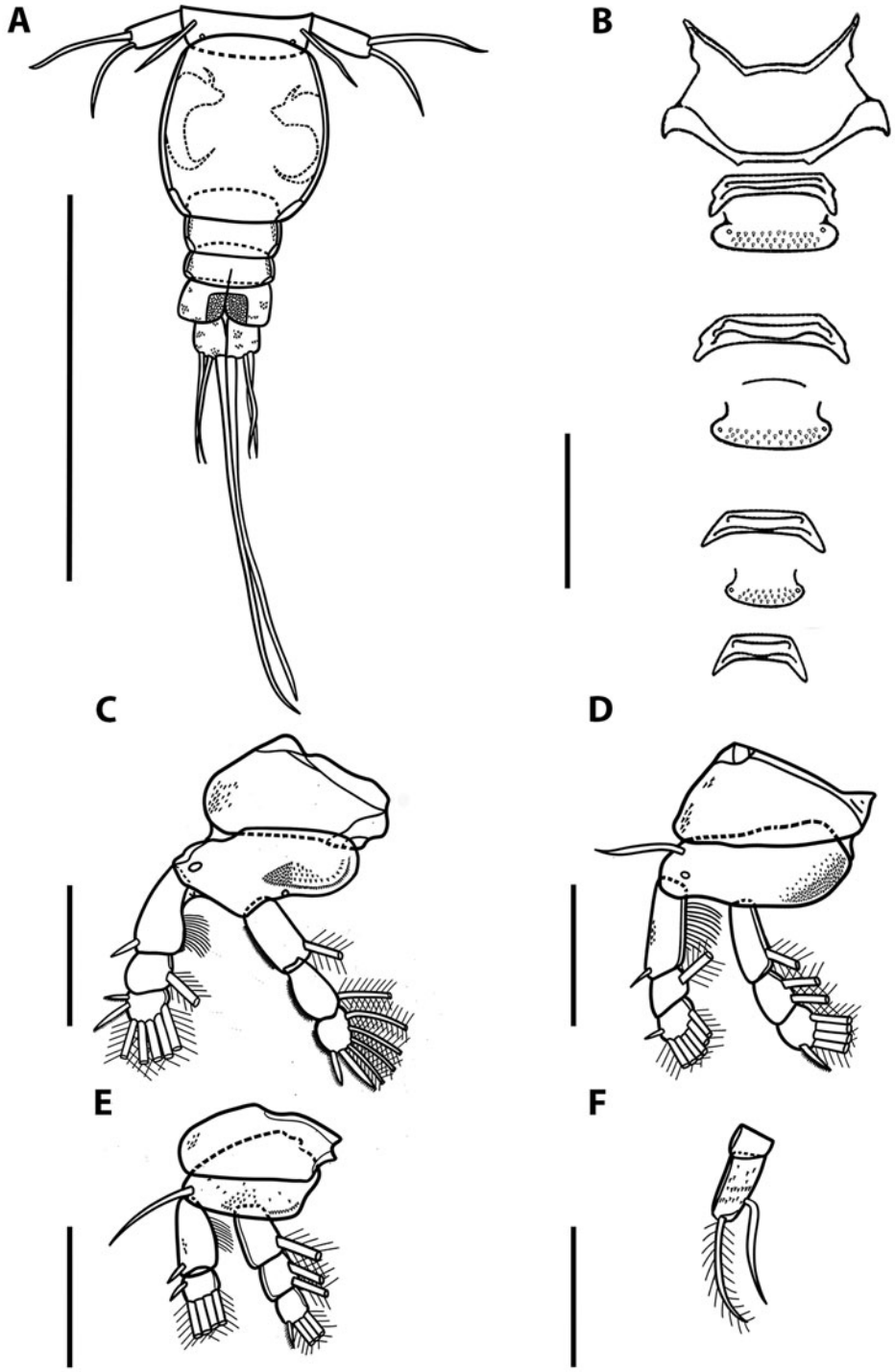

Figure 7. Illustrations of adult female of *Ergasilus chintensis* n. sp: (A) urosome, dorsal view; (B) intercoxal sclerites and interpodal plates; (C) leg 1; (D) leg 2 and leg 3; (E) leg 4; (F) leg 5. Scale bars: A – 200 μm; B – 100 μm; C–F – 50 μm.

comprises prosome, urosome and caudal rami. Prosome composed of cephalosome, fused somites (first to third pedigerous somites) and fourth free somite (Fig. 6A). Cephalosome slightly shorter than wide, oval to trapezoidal, with antennules and antenna visible in dorsal view. Cephalic ornamentation comprising of anterior circular eyespot and an inverted T-structure of thickened chitin situated medially on dorsal side (Fig. 6A and B). Paired sensory pores and papillae observed anterior to eyespot with numerous sensory papillae and pores scattered over the dorsal surface of cephalosome. Rostrum well-developed, with truncated posterior margin. All pedigerous somites wider than long and progressively smaller. Second pedigerous somite 104 (98–110; $n = 2$) long by 292 (287–297; $n = 2$) wide; third pedigerous somite 106 (99–113; $n = 2$) long by 224 (217–231; $n = 2$) wide; fourth pedigerous somite 40 (38–42; $n = 2$) long by 112 (110–114; $n = 2$) wide.

Urosome comprising reduced fifth pedigerous somite, non-pedigerous barrel-shaped genital double somite, and 3 free abdominal somites (Fig. 7A). Reduced fifth pedigerous somite 14 (10–18; $n = 2$) long by 83 (72–94; $n = 2$) wide. Genital double-somite longer, 113 (110–115; $n = 2$), than wide, 88 (86–90; $n = 2$) (Fig. 7A), bearing a pair of multiseriate egg sacs dorsally, measuring 1098 (1101–1095; $n = 2$) long by 190 (192–188; $n = 2$) wide (Fig. 6A). Abdomen 3-segmented, first abdominal somite widest,

https://doi.org/10.1017/S0031182024001550 Published online by Cambridge University Press

Table 6. Spine–setae formula on swimming legs of *Ergasilus chintensis* n. sp.

	Coxa	Basis	Exopod	Endopod
Leg I	0-0	0-0	I-0; 0-1; II-5	0-1; 0-1; II-4
Leg II	0-0	0-1	I-0; 0-1; I-6	0-1; 0-2; I-4
Leg III	0-0	0-1	I-0; 0-1; I-6	0-1; 0-2; I-4
Leg IV	0-0	0-1	I-0; I-4	0-1; 0-2; I-3

Number of spines in Roman numerals, number of setae in Arabic numerals.

28 (24–32; $n = 2$) long by 53 (51–55; $n = 2$) wide, second abdominal somite shorter, 23 (20–25; $n = 2$) long by 50 (49–51; $n = 2$) wide; third somite (= anal somite) incised dorsoventrally (= anal opening or anus) forming attachment for caudal rami, 21 (17–25; $n = 2$) long by 46 (45–47; $n = 2$) wide (Fig. 7A). All abdominal somites with posterior row of ventral spinules.

Caudal rami slightly elongated, 23 (22–25; $n = 2$) long by 18 (17–18; $n = 2$) wide, with 4 setae (Fig. 7A). Innermost seta (IV) longest 184 (182–186; $n = 2$), followed by shortest seta (III) 24 (23–24; $n = 2$) and 2 longer setae (II and I) 55 (54–56; $n = 2$) and 59 (57–60; $n = 2$), respectively (Fig. 7A). Two sensory pores on posterior ventral margins on each ramus.

Antennule 6-segmented, armed with long and short setae (Fig. 6D). Setal formula from proximal to distal segments given as 3–10–6–3–2–6 (total 30). Antenna 4-segmented, comprising of coxobasis, 99 (97–101; $n = 2$) long by 61 (58–65; $n = 2$) wide; and 3-segmented endopod, armed with curved terminal claw (Fig. 6E). First endopod segment longest 182 (181–184; $n = 2$), followed by second endopod segment 110 (108–112; $n = 2$), and small third endopod segment 14 (13–15; $n = 2$). Two spines observed on second endopod segment. Terminal claw pointed and smooth 83 (81–85; $n = 2$), with fossa on inner margin (Fig. 6E).

Mouth positioned ventrally on cephalosome. Mandible armed with 3 blades (anterior, medial and posterior blades); anterior blade thinner and shorter than others, ornamented along anterior margin; medial and posterior blades, both with teeth on opposite margin (Fig. 6C). Maxillule armed with 2 bare setae. Maxilla 2-segmented, comprising syncoxa (= first segment) and basis (= second segment); syncoxa broad with large maxillary pore; basis distally ornamented with numerous teeth on convex margin. Labium broad, unornamented; mid-region produced posteriorly, with rounded posterior margin.

Swimming legs I to IV; each comprising coxa, basis and 2 segmented rami (i.e. exopod, endopod). Rami of all legs 3-segmented, except 2-segmented exopod of leg IV. Segments distinct, typical with similar basic morphology as in other species of *Ergasilus*. Armature on rami as follows (Roman and Arabic numerals indicating spines and plumose setae, respectively) in Table 6.

Leg I (Fig. 7C). Coxa ornamented with spinules on outer margin. Basis lacking outer setae, ornamented with spinules on inner margin. Exopod 3-segmented; first segment with small outer spine; second segment with 1 inner plumose seta, lacking spine; third segment with small spine on outer corner, longer apical spine; both spines with serrated margins; and 5 plumose setae. Endopod 3-segmented; first and second segment each with 1 plumose seta; third segment with 4 plumose setae and 2 distal serrated spines.

Leg II (Fig. 7D). Coxa ornamented with spinules on outer margin. Basis with outer seta and pore, ornamented with multiple spinules on inner margin. Exopod 3-segmented; first segment with small outer spine; second segment with 1 plumose seta, lacking spine; third segment with small spine on outer corner and 6 plumose setae. Endopod 3-segmented; first segment with 1 plumose seta; second segment with 2 plumose setae; third segment with 4 plumose setae and 1 distal serrated spine (Fig. 7D). Leg III (Fig. 7D) with same ornamentation and armament described for leg 2.

Leg IV (Fig. 7E). Coxa ornamented with spinules on outer margin. Basis with outer seta, ornamented with multiple spinules on inner margin. Exopod 2-segmented; first segment with small outer spine; second segment with small spine on outer corner and 4 plumose setae. Endopod 3-segmented; first segment with 1 plumose seta; second segment with 2 plumose setae; third segment with 3 plumose setae and 1 distal serrated spine.

Leg V (Fig. 7F) with single ramus. Ramus 2-segmented: proximal segment rectangular, without any armaments or ornaments; distal segment about 2.5 times longer than previous segment, with spinules scattered across surface, bearing 2 setae (lateral and inner setae); lateral seta plumose.

Intercoxal sclerites of all legs, present (Figs 6A and 7B); each sclerite with both ends directed posteriorly. Interpodal plates of leg I to III ornamented with spinules; fourth plate absent (Fig. 7B).

Remarks

The detailed description of *E. chintensis* n. sp. highlights its unique characteristics among *Ergasilus* species worldwide, especially compared to marine congeners from these geographic regions. Notably, similar to *E. arenalbus* n. sp., its body size averaging 1035 µm sets it apart from both larger species like *E. felichthys* and *E. youngi*, ranging around 1400 µm, and also from species with smaller sizes below 1054 µm, such as *E. atafonensis*, *E. bahiensis*, *E. caraguatatubensis*, *E. ilani*, *E. myctarothes*, *E. parvitergum*, *E. rostralis* and *E. uniseriatus*. Similarities emerge due to their shared size range when comparing the 2 newly described South African species; however, subtle proportional variations in body segments and appendages are key to their differentiation upon closer examination. Additionally, *E. chintensis* n. sp. displays a more intricate armature on its antenna segments than *E. arenalbus* n. sp., where the second endopod segment in this species shows 2 developed spines rather than just 1 as present in *E. arenalbus* n. sp. The most striking feature of *E. chintensis* n. sp. is its body segmentation, characterized by a fused 2-segmented prosome. This completely contrasts with the free prosome somites observed not only in *E. arenalbus* n. sp. but also concerning all the other compared marine ergasilid species. *Ergasilus caraguatatubensis* also exhibits a fused prosome structure, although, to a lesser degree than *E. chintensis* n. sp. The antennule setae formula also contributes to this distinction, with *E. chintensis* n. sp. differing from *E. ilani*, *E. rostralis* and *E. uniseriatus* in antennule segmentation (6- *vs* 5-segmented). These distinguishing features collectively characterize *E. chintensis* n. sp. within the *Ergasilus* genus, highlighting body segmentation, appendage armature and ornamentation as key characteristics for species differentiation.

Molecular characterization and phylogenetic position of African marine Ergasilus *species*

The molecular analyses revealed distinct genetic profiles for the newly described *Ergasilus* species. This study successfully generated a total of 8 sequences. For *E. arenalbus* n. sp., 5 sequences were produced: 2 18S, 2 28S and 1 COI sequence. For *E. chintensis* n. sp., 3 sequences were obtained: 1 18S, 1 28S and 1 COI sequence. Nucleotide comparisons of the 2 new species against the partial 18S rDNA, 28S rDNA and COI mtDNA gene sequences of the genus *Ergasilus* were performed, as detailed in Tables 7–9, respectively. Both ML and BI analyses were conducted on the partial 18S rDNA, 28S rDNA and COI gene alignments, producing phylogenetic trees with congruent topologies. Thus,

https://doi.org/10.1017/S0031182024001550 Published online by Cambridge University Press

Table 7. Nucleotide comparison of the partial 18S rDNA sequences of the genus *Ergasilus* Nordman, 1832, based on 1354 bp-long alignment.

Number of bases/residues which are not identical																			
	E. arenalbus	*E. chintensis*	*E. caparti*	*E. parvus*	*E. macrodactylus*	*E. megacheir*	*E. parasarsi*	*E. sieboldi*	*E. mirabilis*	*E. hypomesi*	*E. tumidus*	*E. briani*	*E. anchoratus*	*E. yaluzangbus*	*E. wilsoni*	*E. parasiluri*	*E. peregrinus*	*E. scalaris*	*P. nana*
E. arenalbus		0	14	14	14	15	15	15	15	19	23	23	25	26	26	27	31	33	99
E. chintensis	100		14	14	14	15	15	16	17	20	24	24	26	30	27	29	32	35	103
E. caparti	98.60	98.60		0	0	1	1	14	3	12	19	19	14	16	18	24	27	19	76
E. parvus	98.60	98.60	100		0	1	1	14	3	12	19	19	14	16	18	24	27	19	76
E. macrodactylus	98.60	98.60	100	100		1	1	14	3	12	19	19	14	16	18	24	27	19	76
E. megacheir	98.50	98.50	99.90	99.90	99.90		0	13	4	13	20	20	15	15	19	25	28	20	76
E. parasarsi	98.50	98.50	99.90	99.90	99.90	100		13	4	13	20	20	15	15	19	25	28	20	76
E. sieboldi	98.87	98.82	98.59	98.59	98.59	98.69	98.69		13	19	21	21	24	23	24	28	33	32	100
E. mirabilis	98.87	98.74	99.70	99.70	99.70	99.60	99.60	99.04		20	22	22	24	23	25	29	36	32	102
E. hypomesi	98.57	98.52	98.80	98.80	98.80	98.69	98.69	98.59	98.52		14	14	24	34	30	20	31	35	104
E. tumidus	98.27	98.23	98.09	98.09	98.09	97.99	97.99	98.45	98.37	98.96		4	31	36	30	20	36	41	106
E. briani	98.27	98.23	98.09	98.09	98.09	97.99	97.99	98.45	98.37	98.96	99.70		31	36	30	20	37	41	106
E. anchoratus	98.12	98.08	98.59	98.59	98.59	98.49	98.49	98.22	98.22	98.22	97.71	97.71		37	37	34	39	28	105
E. yaluzangbus	98.05	97.78	98.39	98.39	98.39	98.49	98.49	98.30	98.30	97.49	97.34	97.34	97.26		33	39	39	45	103
E. wilsoni	98.05	98.00	98.19	98.19	98.19	98.09	98.09	98.22	98.15	97.78	97.78	97.78	97.26	97.56		38	42	49	108
E. parasiluri	97.98	97.86	97.59	97.59	97.59	97.49	97.49	97.93	97.86	98.52	98.52	98.52	97.49	97.12	97.19		42	44	110
E. peregrinus	97.67	97.63	97.29	97.29	97.29	97.19	97.19	97.56	97.34	97.71	97.34	97.26	97.11	97.12	96.89	96.89		50	107
E. scalaris	97.52	97.41	98.09	98.09	98.09	97.99	97.99	97.63	97.63	97.41	96.97	96.97	97.93	96.67	96.37	96.75	96.3		116
P. nana	92.58	92.39	92.38	92.38	92.38	92.38	92.38	92.61	92.47	92.32	92.17	92.17	92.25	92.39	92.02	91.88	92.1	91.4	
Percentage of basis/residues which are identical																			

Table 8. Nucleotide comparison of the partial 28S rDNA sequences of genus *Ergasilus* Nordman, 1832, based on 682 bp-long alignment

Number of bases/residues which are not identical																			
	E. arenalbus	*E. chintensis*	*E. wilsoni*	*E. hypomesi*	*E. peregrinus*	*E. sieboldi*	*E. briani*	*E. tumidus*	*E. scalaris*	*E. parasiluri*	*E. caparti*	*E. megacheir*	*E. macrodactylus*	*E. anchoratus*	*E. parvus*	*E. mirabiis*	*E. parasarsi*	*E. yaluzangbus*	*P. nana*
E. arenalbus		6	37	37	38	48	50	54	55	55	61	62	63	66	68	69	70	71	176
E. chintensis	99.10		36	38	40	46	47	50	54	54	61	62	63	66	68	65	72	72	176
E. wilsoni	94.46	94.61		38	40	42	37	40	42	44	66	66	67	66	70	69	73	70	171
E. hypomesi	94.47	94.32	94.32		40	36	32	35	34	32	55	62	59	67	63	61	60	64	169
E. peregrinus	94.31	94.01	94.01	94.02		44	42	45	46	44	56	57	56	66	59	60	64	64	168
E. sieboldi	92.55	92.86	93.48	94.41	93.17		40	41	43	43	65	72	70	72	74	62	75	66	168
E. briani	92.53	92.97	94.47	95.22	93.72	93.8		19	22	18	65	67	64	77	68	64	69	75	169
E. tumidus	91.93	92.53	94.02	94.78	93.27	93.64	97.16		29	25	67	70	66	80	70	65	72	72	168
E. scalaris	91.77	91.92	93.71	94.92	93.11	93.32	96.71	95.67		8	71	74	71	79	73	76	72	70	173
E. parasiluri	91.77	91.92	93.41	95.22	93.41	93.32	97.31	96.26	98.80		70	73	70	80	70	70	69	72	167
E. caparti	90.67	90.67	89.91	91.59	91.44	89.83	90.08	89.77	89.14	89.30		14	13	78	17	32	18	73	180
E. megacheir	90.52	90.52	89.91	90.52	91.28	88.73	89.77	89.31	88.69	88.84	97.86		9	81	13	41	19	73	180
E. macrodactylus	90.37	90.37	89.76	90.98	91.44	89.05	90.23	89.92	89.14	89.30	98.01	98.62		81	6	43	15	71	177
E. anchoratus	90.13	90.13	90.13	90.00	90.13	88.82	88.51	88.06	88.19	88.04	88.07	87.61	87.61		85	84	85	95	180
E. parvus	89.60	89.60	89.30	90.37	90.98	88.42	89.62	89.31	88.84	89.30	97.40	98.01	99.08	87.00		45	15	74	180
E. mirabilis	89.69	90.28	89.69	90.88	91.03	90.37	90.45	90.30	88.64	89.54	95.10	93.72	93.42	87.44	93.11		44	81	176
E. parasarsi	89.30	88.99	88.84	90.83	90.21	88.26	89.47	89.01	88.99	89.45	97.24	97.09	97.70	87.00	97.70	93.26		70	177
E. yaluzangbus	89.47	89.32	89.61	90.50	90.50	89.81	88.89	89.33	89.61	89.32	88.91	88.91	89.21	85.93	88.75	87.96	89.36		174
P. nana	74.00	74.00	74.74	75.07	75.18	74.27	75.07	75.22	74.45	75.33	72.85	72.85	73.30	73.45	72.85	74.04	73.30	74.37	
Percentage of basis/ residues which are identical																			

Table 9. Nucleotide comparison of the mtDNA COI gene sequences of genus *Ergasilus* Nordman, 1832, based on 700 bp-long alignment.

Number of bases/residues which are not identical							
	E. arenalbus	*E. chintensis*	*E. wilsoni*	*E. auritus*	*E. lizae*	*E. mirabilis*	*P. nana*
E. arenalbus		43	111	119	128	139	177
E. chintensis	93.78		114	123	134	137	179
E. wilsoni	80.93	80.41		111	114	122	146
E. auritus	81.91	81.31	80.93		133	141	177
E. lizae	80.55	79.64	80.41	79.79		130	181
E. mirabilis	79.94	80.17	79.04	78.57	80.24		184
P. nana	74.46	74.36	74.91	73.10	72.49	73.45	
Percentage of basis/residues which are identical							

only the ML tree of the 28S and COI gene regions are presented (Figs 8 and 9, respectively).

The 18S phylogenetic analyses yielded a final alignment consisting of 1354 bases. The 18S sequences exhibited no interspecific variability (0 bp difference) since no differences were found among the 18S rDNA sequences of *E. arenalbus* n. sp. and *E. chintensis* n. sp. (Table 7). The analysis revealed *E. scalaris* Markevich, 1940, as the most genetically distant species from *E. arenalbus* n. sp. (33 bp/2.48%) and *E. chintensis* n. sp. (35 bp/2.59%) (Table 7). The lowest interspecific differences (1.13–1.18%) were observed between the new species and *E. sieboldi* von Nordmann, 1832 (Table 7).

The 28S phylogenetic analysis produced a final alignment of 682 bases. These 28S sequences displayed minor interspecific variability (6 bp) among the 28S rDNA sequences of *E. arenalbus* n. sp. and *E. chintensis* n. sp. (Table 8). The analysis showed *E. parasarsi* Míč *et al.*, 2023, and *E. yaluzangbus* Kuang and Qian, 1985, as the most genetically distant species from *E. arenalbus* n. sp. (71 bp/10.70%) and *E. chintensis* n. sp. (72 bp/10.68%), respectively (Table 8). The smallest interspecific differences (5.39–5.60%) were noted between the new species and *E. wilsoni* Markevich, 1933 (Table 8). ML and BI analyses using rDNA alignment that included partial 28S sequences of Ergasilidae produced trees with consistent topologies and similar nodal support values.

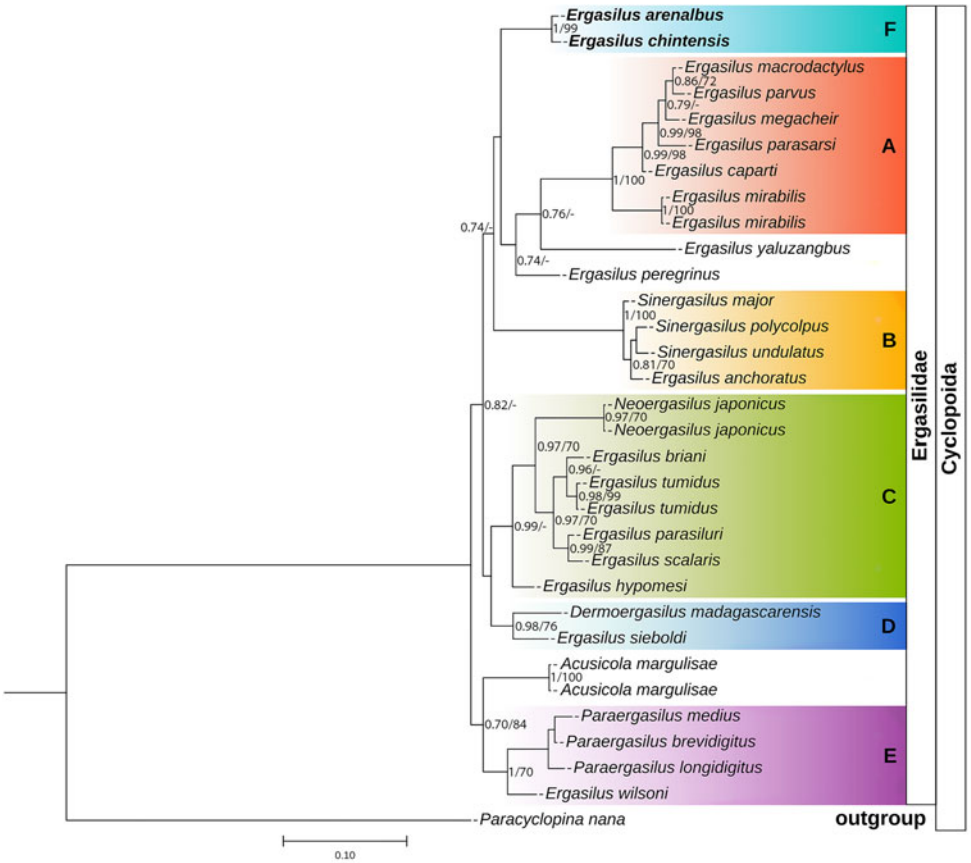

Figure 8. Phylogenetic tree of Ergasilidae copepods based on partial 28S rRNA gene alignments. Newly generated sequences for *Ergasilus arenalbus* n. sp. and *Ergasilus chintensis* n. sp. are provided in bold. Nodal support presented above or below branches for Bayesian Inference (>0.7) and Maximum Likelihood (>70%) analyses (BI/ML). Dashes indicate values below 0.7 and 70%, respectively. *Paracyclopina nana* Smirnov, 1935, was used as the outgroup.

https://doi.org/10.1017/S0031182024001550 Published online by Cambridge University Press

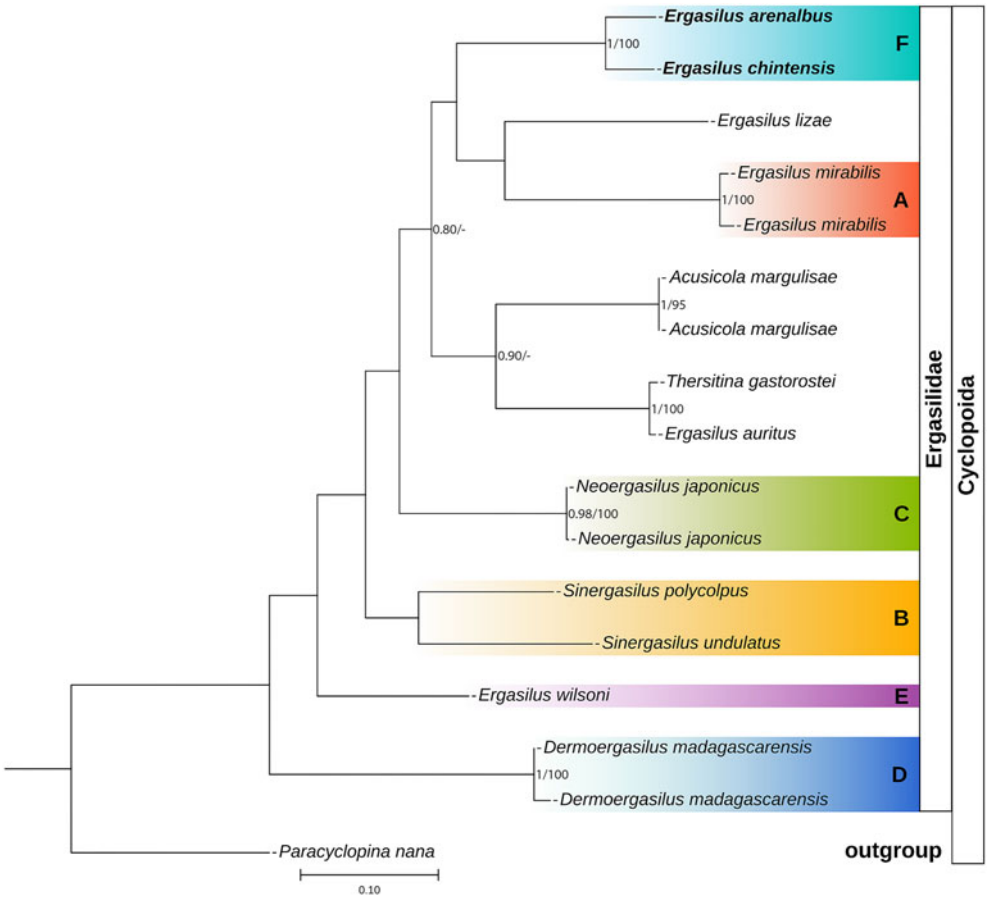

Figure 9. Phylogenetic tree of Ergasilidae copepods based on partial COI mtDNA gene alignments. Newly generated sequences for *Ergasilus arenalbus* n. sp. and *Ergasilus chintensis* n. sp. are provided in bold. Nodal support presented above or below branches for Bayesian Inference (>0.7) and Maximum Likelihood (>70%) analyses (BI/ML). Dashes indicate values below 0.7 and 70%, respectively. *Paracyclopina nana* Smirnov, 1935, was used as the outgroup.

Consistent with previous phylogenetic studies on ergasilids (Song *et al.*, 2008; Santacruz *et al.*, 2020; Fikiye *et al.*, 2023; Míč *et al.*, 2023, 2024), the analyses identified 5 well-supported polyphyletic *Ergasilus* groups (Fig. 8): (A) the African freshwater *Ergasilus* species, (B) the *Sinergasilus* Yin, 1949, species and the *E. anchoratus* Markevich, 1946, group, (C) the Asian *Ergasilus* species and the *Neoergasilus japonicus* (Harada, 1930) group, (D) the recently described *Dermoergasilus madagascarensis* Míč *et al.* , 2024, and *E. sieboldi* group and (E) the *Paraergasilus* Markevich, 1937, species and the *E. wilsoni* group (Fig. 8). Despite forming a distinct subclade (F), the newly described species still clustered within the larger clade that includes subclade (A) comprising African freshwater species, along with non-African species like *E. yaluzangbus* and *E. peregrinus* Heller, 1865 (Fig. 8).

COI sequences were aligned using invertebrate mitochondrial translation, resulting in an alignment length of 700 bases. The sequences included GenBank and BOLD sequences submitted from Canada (Table 4). These results displayed substantial interspecific variability (43 bp) among the COI sequences of *E. arenalbus* n. sp. and *E. chintensis* n. sp. and more than 110 bases from all other *Ergasilus* congeners (Table 9). The analysis showed *E. mirabilis* Oldewage and van As, 1987, and *E. lizae* as the most genetically distant species from *E. arenalbus* n. sp. (139 bp/20.06%) and *E. chintensis* n. sp. (134 bp/20.36%), respectively (Table 9). The smallest interspecific differences (19.07–19.59%) were noted between the new species and *E. wilsoni* (Table 9). Similar to the 28S tree topology, the novel sequences of *E. arenalbus* n. sp. and *E. chintensis* n. sp. formed the same subclade (F), within the larger clade that includes subclade (A) comprising African freshwater species, *E. mirabilis*, and the morphologically similar marine species *E. lizae*, which is also found within the Indian Ocean (Fig. 9).

Based on these analyses, this study proposes the existence of a sixth clade (F) consisting of African marine *Ergasilus* species (Figs 8 and 9). However, this proposition remains speculative as their precise phylogenetic placement within Ergasilidae remains unresolved due to low support values and limited molecular data, concerning marine ergasilids.

Discussion

The discovery of 2 new *Ergasilus* species, *E. arenalbus* n. sp. and *E. chintensis* n. sp., from the Evileye blaasop, *A. honckenii*, significantly enhances our understanding of marine parasite diversity in South Africa. These findings highlight the underexplored nature of marine parasites in this region, particularly within the genus *Ergasilus*, known for its rich diversity in global freshwater and marine environments (Boxshall and Defaye, 2008; Fikiye *et al.*, 2023; Míč *et al.*, 2023). To date, only a limited number of *Ergasilus* species have been reported from African marine environments, with only 5 documented, including just 1 from South Africa (Fikiye *et al.*, 2023; WoRMS, 2024). Moreover, despite *Ergasilus* being found in a wide range of fish host families (see Table 1), only a single species, *E. colomesus* Thatcher and Boeger, 1983, has been described from the family Tetraodontidae Bonaparte, 1832 (Thatcher and Boeger, 1983) in the Amazon River, Brazil.

https://doi.org/10.1017/S0031182024001550 Published online by Cambridge University Press

The addition of *E. arenalbus* n. sp. and *E. chintensis* n. sp. not only introduces new host records but also suggests a higher hidden diversity of *Ergasilus* within South Africa's coastal region and the Tetraodontidae family. This hints at a potentially broader copepod diversity and novel host–parasite relationships yet to be explored, aligning with global trends revealing extensive species diversity in under-studied marine ecosystems (Boxshall and Defaye, 2008). The presence of these new species along the South African coastline highlights the region's rich marine biodiversity and emphasizes the importance of investigating lesser-known areas and hosts for hidden parasite diversity.

Taxonomically, detailed morphological examinations of these species, focusing on size, body segmentation, appendage armature and ornamentation, provide crucial insights into their distinctiveness from known congeners. Integrating traditional morphological taxonomy with molecular techniques has been instrumental in characterizing these new *Ergasilus* species. Molecular analyses alongside morphological assessments confirm the uniqueness of these species with greater accuracy (Míč *et al.*, 2024; Walter and Boxshall, 2024). This integration is valuable as morphological characters alone often yield conflicting results in distinguishing new species and understanding their placement within Ergasilidae lineages (Míč *et al.*, 2024; Walter and Boxshall, 2024).

The nomenclatural history of ergasilids emphasizes the significant challenge of formulating generic diagnoses that effectively distinguish species. This complexity is evidenced by the synonymization of 33 *Ergasilus* species either with other previously described *Ergasilus* species or with species from different genera within the Ergasilidae family (Walter and Boxshall, 2024). Moreover, genera such as *Acusicola* Cressey, in Cressey and Collette, 1970, *Dermoergasilus* Ho and Do, 1982, *Neoergasilus* Yin, 1956, *Paraergasilus* and *Sinergasilus*, have consistently been confirmed as monophyletic (Song *et al.*, 2008; Santacruz *et al.*, 2020; Kvach *et al.*, 2021; Míč *et al.*, 2023, 2024). However, these genera render *Ergasilus* polyphyletic, with certain species, like *E. anchoratus*, *E. sieboldi* and *E. wilsoni*, showing closer relationships to *Sinergasilus*, *Dermoergasilus* and *Paraergasilus*, respectively (Figs 8 and 9).

Phylogenetics pose significant challenges that hinder comprehensive genomic analyses of *Ergasilus* species, creating obstacles in gaining deeper insights into their biology. The limited knowledge regarding their diversity and the lack of genetic data, compared to those of other well-studied organisms, are major contributing factors. Previous studies (Song *et al.*, 2008; Santacruz *et al.*, 2020; Kvach *et al.*, 2021; Míč *et al.*, 2023, 2024) have attempted to overcome these challenges through molecular characterization using rRNA genes, particularly the 18S and 28S rDNA regions. However, the effectiveness of these markers in species-level differentiation has been variable (Míč *et al.*, 2023, 2024). The 18S rDNA region of the present study has shown minimal or even zero variation (0–2.59%) in some cases, making it unsuitable for distinguishing between closely related species. This is consistent with findings from earlier studies, which reported that the 18S rRNA gene is highly conserved and not suitable for identification at lower taxonomic levels (Taniguchi *et al.*, 2004; Huys *et al.*, 2006; Tang *et al.*, 2012; Marrone *et al.*, 2013). This lack of variation reinforces the limitations of the 18S rDNA marker for species-level differentiation within this genus.

In contrast, the 28S rDNA analyses have proven more effective in distinguishing between species (Song *et al.*, 2008; Santacruz *et al.*, 2020; Kvach *et al.*, 2021; Míč *et al.*, 2023, 2024). The present study supports these findings to an extent, revealing higher, albeit minor interspecific divergence (6 bp between *E. arenalbus* n. sp. and *E. chintensis* n. sp.). The analysis also identified other *Ergasilus* species as genetically distant from the newly described taxa, highlighting the potential of 28S rDNA in elucidating phylogenetic relationships within the family Ergasilidae. However, despite its relative effectiveness, the genetic variation observed in the 28S rDNA is still limited, with little variation (0.90–10.70%), compared to other markers, raising questions about its adequacy for reliable species identification.

The COI gene, a widely used barcode for species-level differentiation (Tang *et al.*, 2012; Baek *et al.*, 2016; Mayor *et al.*, 2017; Míč *et al.*, 2023, 2024), demonstrated high resolution at the species level for the *Ergasilus* species described in this study and indicated significant interspecific variability. The COI analyses revealed substantial differences (43 bp) among the COI sequences of *E. arenalbus* n. sp. and *E. chintensis* n. sp., as well as notable variation from other *Ergasilus* congeners. This suggests that the COI gene may be a more suitable marker for species-level differentiation in this group. However, it is important to note that the limited availability of only 4 other *Ergasilus* COI sequences (see Fig. 9 and Table 9) means that drawing definitive conclusions from these results is premature. While COI shows promise for more precise species identification, further research is needed to expand the dataset and validate its effectiveness across a broader range of *Ergasilus* species. Moving forward, prioritizing the COI gene in future studies may provide a clearer understanding of the diversity and evolutionary relationships within the family Ergasilidae.

The phylogenetic relationships of ergasilid copepods remain largely unclear, with only 11% (31 out of 277) of the known species with any molecular data available (Míč *et al.*, 2023, 2024; Walter and Boxshall, 2024). Limited studies have examined the genetic characteristics of African *Ergasilus* species (Fikiye *et al.*, 2023, Míč *et al.*, 2023), and no genetic studies exist for the characterization of marine species. Notably, the present study provides the first marine sequences for this genus. The only available brackish sequences are for *Ergasilus wilsoni* and *Ergasilus sieboldi* (Walter and Boxshall, 2024), both of which are primarily associated with freshwater environments rather than being strictly marine or brackish. *Ergasilus wilsoni* and *E. sieboldi* can inhabit fresh or brackish waters, while recognized as typical freshwater species found in the Palearctic region, particularly in rivers and lakes (Kvach *et al.*, 2021), distinguishing them from the newly discovered *Ergasilus* species, as close relationships among ergasilids may be influenced by the geographical origin of the species or the endemism of their hosts (Míč *et al.*, 2023). This means that parasite distribution is closely linked to the geographic distribution of their hosts (Morand and Guégan, 2000), suggesting potential coevolution between parasites and hosts. The discovery of 2 genetically similar species from the same host species suggests that the 2 newly identified *Ergasilus* species associated with pufferfish along the South African coast reflect coevolutionary patterns and host-specific endemism. These findings are consistent with conclusions drawn from previous phylogenetic studies (Song *et al.*, 2008; Santacruz *et al.*, 2020; Kvach *et al.*, 2021; Oliveira *et al.*, 2021). Therefore, the geographic separation between *E. sieboldi* and *E. wilsoni* from the newly discovered species further highlights the critical need for more comprehensive genetic data on marine *Ergasilus* species to enhance our understanding of their diversity, evolutionary relationships and distribution patterns.

Conclusion

The discovery and descriptions of *E. arenalbus* n. sp. and *E. chintensis* n. sp. in association with the Evileye blaasop represent a significant advance in our understanding of marine parasite diversity in South Africa. These results highlight the rich marine ecosystems of the region and emphasize the importance of investigating

https://doi.org/10.1017/S0031182024001550 Published online by Cambridge University Press

under-explored areas to uncover the hidden biodiversity. Furthermore, the new *Ergasilus* sequences and phylogenetic analyses presented in this study provide the first insight into the phylogenetic relationships of marine *Ergasilus* species within the South Atlantic and Indian Ocean regions. Alongside the studies by Míč *et al.* (2023, 2024) and Fikiye *et al.* (2023), this research also offers a further understanding of the African clade lineage, making the molecular data presented here the first to elucidate the phylogenetic relationships of this genus in African and marine systems. Our phylogenetic analysis suggests that African marine ergasilids form a distinct monophyletic lineage separate from freshwater species, proposing the recognition of a sixth clade (F) for African marine *Ergasilus* species (Figs 8 and 9). Nonetheless, due to low support values and the scarcity of molecular data for marine ergasilids, their exact phylogenetic placement within the family Ergasilidae remains unresolved. Further studies that integrate both morphological and molecular data are essential to elucidate these relationships.

Data available statement. Sequence data are available on the NCBIGenBank database. All other necessary data are included in the article.

Acknowledgements. We would like to thank the Unit for Environmental Sciences and Management, North-West University (NWU) for the use of field equipment and laboratory facilities. We thank Anja Erasmus from NWU-WRG, for the creation of the study area map. Additional thanks go to our colleagues Francois Retief, Reese Alberts, Anja Erasmus, Marliese Truter, Anja Vermaak and Coret van Wyk, from the NWU who assisted with the collection of samples. This is contribution No. 920 from the NWU-Water Research Group.

Author contributions. L. van der Spuy: methodology, investigation, funding acquisition, writing – original draft. R. B. Narciso: methodology, investigation, drawing, writing – review and editing. K. A. Hadfield: methodology, funding acquisition, writing – review and editing. V. Wepener: conceptualization, data curation, funding acquisition, writing – review and editing. N. J. Smit: conceptualization, data curation, funding acquisition, writing – review and editing.

Financial support. This work is based on the research supported by the National Research Foundation (NRF) of South Africa (grant 132805; L. van der Spuy; grant 150623; N. J. Smit). Opinions, findings, conclusions and recommendations expressed in this publication are those of the authors, and the NRF accept no liability whatsoever in this regard. The authors acknowledge The Nippon Foundation-Nekton Ocean Census Programme (https://oceancensus.org/) for supporting the description of these species. These are Ocean Census Species Numbers 49–50.

Competing interests. The authors declare that they have no known competing financial interests or personal relationships that could have appeared to influence the work reported in this paper.

References

Amado MAPM and Rocha CEF (1996) Three new species of parasitic copepods of the genus *Ergasilus* (Poecilostomatoida, Ergasilidae) collected from the branchial filaments of the mugilid fishes in Brazil. *Nauplius, Rio Grande* **3**, 33–48.

Baek SY, Jang KH, Choi EH, Ryu SH, Kim SK, Lee JH, Lim YJ, Lee J, Jun J, Kwak M, Lee YS, Hwang JS, Maran BAV, Chang CY, Kim IH and Hwang UW (2016) DNA barcoding of metazoan zooplankton copepods from South Korea. *PLoS ONE* **11**, e157307. doi: 10.1371/journal.pone.0157307.

Barcode of Life Database, BOLD SYSTEMS. Available at http://www.boldsystems.org/index.php/TaxBrowser_TaxonPage?taxid=598126 (accessed 7 June 2023).

Beneden E (1870) Recherches sur la composition et la signification de l'oeuf, basées sur l'étude de son mode de formation et des premiers phénomènes embryonnaires (Mammifères, Oiseaux, Crustacés, Vers). *Mémoires Couronnes et Mémoires des Savants Étrangers de l'Académie Royale des Sciences de Belgique* **34**, 1–283.

Bianchini G and Sánchez-Baracaldo P (2024) Treeviewer: flexible, modular software to visualise and manipulate phylogenetic trees. *Ecology and Evolution* **14**, e10873. doi: 10.1002/ece3.10873.

Boxshall GA and Defaye D (2008) Global diversity of copepods (Crustacea: Copepoda) in freshwater. *Hydrobiologia* **595**, 195–207. doi: 10.1007/s10750-007-9014-4.

Boxshall GA and Halsey SH (2004) *An Introduction to Copepod Diversity*. London: The Ray Society.

Boxshall GA and Montú MA (1997) Copepods parasitic on Brazilian coastal fishes: a handbook. *Nauplius* **5**, 1–225.

Boxshall GA, Araujo HMP and Montu M (2002) A new species of *Ergasilus* Nordmann, 1832 (Copepoda, Ergasilidae) from Brazil. *Crustaceana Leiden* **75**, 269–276.

Byrnes TB (1986) Some ergasilids (Copepoda) parasitic on four species of Australian bream, *Acanthopagrus* spp. *Australian Journal of Marine and Freshwater Research* **37**, 81–93. doi: 10.1071/MF9860081.

Carvalho J (1955) *Ergasilus xenomelanirisi* n. sp. parasito de Peixe-Rei: *Xenomelaniris brasiliensis* (Quoy & Gaimard) (Copepoda - Cyclopoida - Pisces - Mugiloidei). *Boletim do Instituto Oceanográfico* **6**, 215–226.

Carvalho J (1962) *Ergasilus* cyanopictus sp. nov, parasito da Tainha – *Mugil cephalus* (L.). *Archivos do Museu Nacional do Rio de Janeiro* **52**, 31–36.

Darriba D, Taboada GL, Doallo R and Posada D (2012) Jmodeltest 2: more models, new heuristics and parallel computing. *Nature Methods* **9**, 772. doi: 10.1038/nmeth.2109.

Dos Santos QM, Avenant-Oldewage A, Piasecki W, Molnar K, Sellyei B and Szekely C (2021) An alien parasite affects local fauna: confirmation of *Sinergasilus major* (Copepoda: Ergasilidae) switching hosts and infecting native *Silurus glanis* (Actinopterygii: Siluridae) in Hungary. *International Journal for Parasitology: Parasites and Wildlife* **15**, 127–131. doi: 10.1016/j.ijppaw.2021.04.011.

El-Rashidy HH and Boxshall GA (2002) New species and new records of *Ergasilus* Nordmann (Copepoda: Ergasilidae) from the gills of grey mullet (Mugilidae). *Systematic Parasitology* **51**, 37–58.

Everett B, Groeneveld J, Fennessy S, Porter S, Munga C, Dias N, Filipe O, Zacarias L, Igulu M, Kuguru B, Kimani E, Rabarison G and Razafindrakoto H (2015) Demersal trawl surveys show ecological gradients in Southwest Indian Ocean slope fauna. *Western Indian Ocean Journal of Marine Science* **14**, 73–92.

Fikiye PP, Smit NJ, Van As LL, Truter M and Hadfield KA (2023) Integrative morphological and genetic characterisation of the fish parasitic copepod *Ergasilus mirabilis* Oldewage & van As, 1987: insights into host specificity and distribution in Southern Africa. *Diversity* **15**, 965. doi: 10.3390/d15090965.

Folmer O, Black M, Hoeh W, Lutz R and Vrijenhoek R (1994) DNA primers for amplification of mitochondrial cytochrome c oxidase subunit I from diverse metazoan invertebrates. *Molecular Marine Biology and Biotechnology* **3**, 294–299, PMID: 7881515.

Fricke R, Eschmeyer WN and Van der Laan R (eds) (2024) Eschmeyer's catalog of fishes: genera, species, references. Available at http://researcharchive.calacademy.org/research/ichthyology/catalog/fishcatmain.asp (accessed 20 July 2024).

Froese R and Pauly D (eds) (2024) FishBase. World Wide Web electronic publication. Available at www.fishbase.org (accessed 20 July 2024).

Guindon S, Dufayard JF, Lefort V, Anisimova M, Hordijk W and Gascuel O (2010) New algorithms and methods to estimate maximum-likelihood phylogenies: assessing the performance of PhyML 3.0. *Systematic Biology* **59**, 307–321. doi: 10.1093/sysbio/syq010.

Ho JS, Jayarajan P and Radhakrishnan S (1992) Copepods of the family Ergasilidae (Poecilostomatoida) parasitic on coastal fishes of Kerala, India. *Journal of Natural History* **26**, 1227–1241. doi: 10.1080/00222939200770691.

Hua CJ, Su MY, Sun ZW, Lu YH and Feng JM (2021) Complete mitochondrial genome of the copepod *Sinergasilus undulatus* (Copepoda: Poecilostomatoida). *Mitochondrial DNA B Resources* **6**, 1226–1228. doi: 10.1080/23802359.2020.1870890.

Huys R, Llewellyn-Hughes J, Olson PD and Nagasawa K (2006) Small subunit rDNA and Bayesian inference reveal *Pectenophilus ornatus* (Copepoda incertae sedis) as highly transformed Mytilicolidae, and support assignment of Chondracanthidae and Xarifiidae to Lichomolgoidea (Cyclopoida). *Biological Journal of the Linnean Society* **87**, 403–425. doi: 10.1111/j.1095-8312.2005.00579.

Jafri SIH (1995) A new copepod parasite, *Ergasilus pakistanicus*, new species (Poecilostomatoida: Ergasilidae) from a freshwater fish in Sindh, Pakistan. *Pakistan Journal of Zoology* **27**, 153–156.

https://doi.org/10.1017/S0031182024001550 Published online by Cambridge University Press

Johnson SK and Rogers WA (1972) *Ergasilus clupeidarum* sp. n. (Copepoda: Cyclopoida) from clupeid fishes of the southeastern U.S. with a synopsis of the North American *Ergasilus* species with a two-jointed first endopod. *Journal of Parasitology* **58**, 385–392.

Kabata Z (1992) Copepoda parasitic on Australian fishes, XV. Family Ergasilidae (Poecilostomatoida). *Journal of Natural History* **26**, 47–66.

Katoh K and Standley M (2013) MAFFT multiple sequence alignment software version 7: improvements in performance and usability. *Molecular Biology and Evolution* **30**, 772–780. doi: 10.1093/molbev/mst010.

Katoh K, Misawa K, Kuma KI and Miyata T (2002) MAFFT: a novel method for rapid multiple sequence alignment based on fast Fourier transform. *Nucleic Acids Research* **30**, 3059–3066. doi: 10.1093/nar/gkf436.

Ki J-S, Park HG and Lee J-S (2009) The complete mitochondrial genome of the cyclopoid copepod *Paracyclopina nana*: a highly divergent genome with novel gene order and atypical gene numbers. *Gene* **435**, 13–22. doi: 10.1016/j.gene.2009.01.005.

Ki JSH, Park G and Lee JS (2011) Extensive analysis of nuclear cistron rDNA sequence of *Paracyclopina nana* (Cyclopoida: Cyclopettidae). *Hydrobiologia* **666**, 3–9. doi: 10.1007/s10750-010-0563-6.

Killian E and Avenant-Oldewage A (2013) Infestation and pathological alterations by *Ergasilus sarsi* (Copepoda) on the Tanganyika killifish from Africa. *Journal of Aquatic Animal Health* **25**, 237–242. doi: 10.1080/08997659.2013.812874.

Kvach Y, Tkachenko MY, Seifertová M and Ondračková M (2021) Insights into the diversity, distribution and phylogeny of three ergasilid copepods (Hexanauplia: Ergasilidae) in lentic water bodies of the Morava River basin, Czech Republic. *Limnologica* **91**, 125922. doi: 10.1016/j.limno.2021.125922.

Marrone F, Lo Brutto S, Hundsdoerfer AK and Arculeo M (2013) Overlooked cryptic endemism in copepods: systematics and natural history of the calanoid subgenus *Occidodiaptomus* Borutzky 1991 (Copepoda, Calanoida. Diaptomidae). *Molecular Phylogenetics and Evolution* **66**, 190–202. doi: 10.1016/j.ympev.2012.09.016.

Mayor TY, Galimova YA, Sheveleva NG, Sukhanova LV and Kirilchik SV (2017) Molecular phylogenetic analysis of *Diacyclops* and *Acanthocyclops* (Copepoda: Cyclopoida) from Lake Baikal based on COI gene. *Russian Journal of Genetics* **53**, 252–258. doi: 10.1134/S1022795417020041.

Míč R, Řehulková E and Seifertová M (2023) Species of *Ergasilus* von Nordmann, 1832 (Copepoda: Ergasilidae) from cichlid fishes in Lake Tanganyika. *Parasitology* **150**, 579–598. doi: 10.1017/S0031182023000239.

Míč R, Řehulková E, Šimková A, Razanabolana JR and Seifertová M (2024) New species of *Dermoergasilus* Ho & Do, 1982 (Copepoda: Cyclopoida: Ergasilidae) parasitizing endemic cichlid *Paretroplus polyactis* (Bleeker) in Madagascar. *Parasitology* **151**, 319–336. doi: 10.1017/S0031182024000088.

Miller M, Pfeiffer WT and Schwartz T (2010) Creating the CIPRES science gateway for inference of large phylogenetic trees. *Proceedings of the Gateway Computing Environments Workshop* **14**, 1–8. doi: 10.1109/GCE.2010.5676129.

Miller EC, Hayashi KT, Song D and Wiens JJ (2018) Explaining the ocean's richest biodiversity hotspot and global patterns of fish diversity. *Proceedings of the Royal Society B: Biological Sciences* **285**, 20181314. doi: 10.1098/rspb.2018.1314.

Morand S and Guégan J-F (2000) Patterns of endemism in host-parasite associations: lessons from epidemiological models and comparative tests. *Belgian Journal of Entomology* **2**, 135–147.

Oldewage WH and Avenant-Oldewage A (1993) Checklist of the parasitic Copepoda (Crustacea) of African fishes. *Koninklijk Museum voor Midden-Afrika – Zoology Documents* **23**, 2–28.

Oldewage WH and van As JG (1988) A key for the identification of African piscine parasitic Ergasilidae (Copepoda:Poecilostomatoida). *South African Journal of Zoology* **23**, 42–46. doi: 10.1080/02541858.1988.11448075.

Oliveira MSB, Corrêa LL, Adriano EA and Tavares-Dias M (2021) Integrative taxonomy of a new species of *Therodamas* (Ergasilidae) infecting the Amazonian freshwater fish *Leporinus fasciatus* (Anostomidae). *Parasitology Research* **120**, 3137–3147. doi: 10.1007/s00436-021-07256-y.

Ondračková M, Fojtu J, Seifertová M, Kvach Y and Jurajda P (2019) Non-native parasitic copepod *Neoergasilus japonicus* (Harada, 1930) utilizes non-native fish host *Lepomis gibbosus* (L.) in the floodplain of the river Dyje (Danube basin). *Parasitology Research* **118**, 57–62. doi: 10.1007/s00436-018-6114-1.

Pearse AS (1947) Parasitic copepods from Beaufort, North Carolina. *Journal of the Elisha Mitchell Scientific Society* **63**, 1–16.

Posada D (2008) Jmodeltest: phylogenetic model averaging. *Molecular Biology and Evolution* **25**, 1253–1256. doi: 10.1093/molbev/msn083.

Redkar MV, Rangnekar PG and Murti NN (1952) *Ergasilus polynemi* sp. nov. (Copepoda) parasitic on the fish *Polynemus tetradactylus* Shaw. *Journal of the Zoological Society of India* **3**, 223–227.

Ronquist F, Teslenko M, van der Mark P, Ayres DL, Darling A, Höhna S, Larget B, Liu L, Suchard MA and Huelsenbeck JP (2012) Mrbayes 3.2: efficient Bayesian phylogenetic inference and model choice across a large model space. *Systematic Biology* **61**, 539–542. doi: 10.1093/sysbio/sys029.

Santacruz A, Morales-Serna FN, Leal-Cardín M, Barluenga M and Pérez-Ponce de León G (2020) *Acusicola margulisae* n. sp. (Copepoda: Ergasilidae) from freshwater fishes in a Nicaraguan crater lake based on morphological and molecular evidence. *Systematic Parasitology* **97**, 165–177. doi: 10.1007/s11230-020-09906-8.

Smith MM and Heemstra PC (2012) *Smith's Sea Fishes*. Heidelburg, Germany: Springer Science & Business Media, 1191 pp.

Song Y, Wang GT, Yao WJ, Gao Q and Nie P (2008) Phylogeny of freshwater parasitic copepods in the Ergasilidae (Copepoda: Poecilostomatoida) based on 18S and 28S rDNA sequences. *Parasitology Research* **102**, 299–306. doi: 10.1007/s00436-007-0764-8.

Tang CQ, Leasi F, Obertegger U, Kieneke A, Barraclough TG and Fontaneto D (2012) The widely used small subunit 18S rDNA molecule greatly underestimates true diversity in biodiversity surveys of the meiofauna. *Proceedings of the National Academy of Sciences* **109**, 16208–16212. doi: 10.1073/pnas.1209160109.

Taniguchi M, Kanehisa T, Sawabe T, Christen R and Ikeda T (2004) Molecular phylogeny of *Neocalanus* copepods in the subarctic Pacific Ocean, with notes on non-geographical genetic variations for *Neocalanus cristatus*. *Journal of Plankton Research* **26**, 1249–1255. doi: 10.1093/plankt/fbh115.

Tavares LER and Luque JL (2005) *Ergasilus youngi* sp. nov. (Copepoda: Poecilostomatoida: Ergasilidae) parasitic on *Aspistor luniscutis* (Actinopterygii: Ariidae) from off the State of Rio de Janeiro, Brazil. *Acta Parasitologica* **50**, 150–155.

Thatcher VE and Boeger WA (1983) The parasitic crustaceans of fishes from the Brazilian Amazon. 4. *Ergasilus colomesus* n. sp. (Copepoda: Cyclopoida) from an ornamental fish, *Colomesus asellus* (Tetraodontidae) and aspects of its pathogenicity. *Transactions of the American Microscopical Society* **102**, 371–379.

Thomas S (1993) A new species of the genus *Ergasilus* Nordmann, 1832 (Copepoda: Poecilostomatoida) from Kerala. *Journal of the Bombay Natural History Society* **90**, 451–454.

Thomsen R (1949) Copépodos parásitos de los peces marinos del Uruguay. *Comunicaciones Zoologicas del Museo de Historia Natural de Montevideo* **3**, 1–41.

Vasquez AA, Bonnici BL, Kashian, R, Trejo-Martinez J, Miller CJ and Ram JL (2023) The biodiversity of freshwater crustaceans revealed by taxonomy and mitochondrial DNA barcodes; Physiology Faculty Research Publications: Wayne State University: Detroit, MI, USA, 2021; Volume 3, Available at https://digitalcommons.wayne.edu/physio_frp/3 (accessed 1 April 2023).

Walter TC and Boxshall G (2024) World of copepods database. *Ergasilus* Nordmann, 1832. Accessed through: World Register of Marine Species. Available at https://www.marinespecies.org/aphia.php?p=taxdetails&id=128641 (accessed 15 May 2024).

Wilson CB (1913) Crustacean parasites of West Indian fishes and land crabs, with description of new genera and species. *Proceedings of the United States National Museum* **44**, 189–277.

WoRMS Editorial Board (2024) World Register of Marine Species. Available at https://www.marinespecies.org at VLIZ. doi: 10.14284/170 (accessed 15 May 2024).